5. Shimizu Y, et al. (2000) Benzopyrene carcinogenicity is lost in mice lacking the aryl hydrocarbon receptor. *Proc Natl Acad Sci USA* 97:779–782.
6. Ohtake F, et al. (2007) Dioxin receptor is a ligand-dependent E3 ubiquitin ligase. *Nature* 446:562–566.
7. Quintana FJ, et al. (2008) Control of T_{reg} and T_H17 cell differentiation by the aryl hydrocarbon receptor. *Nature* 453:65–71.
8. Veldhoen M, et al. (2008) The aryl hydrocarbon receptor links T_H17-cell-mediated autoimmunity to environmental toxins. *Nature* 453:106–109.
9. Kimura A, Naka T, Nohara K, Fujii-Kuriyama Y, Kishimoto T (2008) Aryl hydrocarbon receptor regulates Stat1 activation and participates in the development of Th17 cells. *Proc Natl Acad Sci USA* 105:9721–9726.
10. Ikuta T, Kobayashi Y, Kawajiri K (2004) Cell density regulates intracellular localization of aryl hydrocarbon receptor. *J Biol Chem* 279:19209–19216.
11. Lee S, et al. (1996) Nuclear/cytoplasmic localization of the von Hippel-Lindau tumor suppressor gene product is determined by cell density. *Proc Natl Acad Sci USA* 93:1770–1775.
12. Zhang F, White RL, Neufeld KL (2001) Cell density and phosphorylation control the subcellular localization of adenomatous polyposis coli protein. *Mol Cell Biol* 21:8143–8156.
13. Nguyen LP, Bradfield CA (2008) The search for endogenous activators of the aryl hydrocarbon receptor. *Chem Res Toxicol* 21:102–116.
14. Heath-Pagliuso S, et al. (1998) Activation of the Ah receptor by tryptophan and tryptophan metabolites. *Biochemistry* 37:11508–11515.
15. Bjeldanes LF, et al. (1991) Aromatic hydrocarbon responsiveness-receptor agonists generated from indole-3-carbinol *in vitro* and *in vivo*: Comparisons with 2,3,7,8-tetrachlorodibenzo-*p*-dioxin. *Proc Natl Acad Sci USA* 88:9543–9547.
16. Kim YS, Milner JA (2005) Targets for indole-3-carbinol in cancer prevention. *J Nut Biochem* 16:65–73.
17. Bonnesen C, Eggleston IM, Hayes JD (2001) Dietary indoles and isothiocyanates that are generated from cruciferous vegetables can both stimulate apoptosis and confer protection against DNA damage in human colon cell lines. *Cancer Res* 61:6120–6130.
18. Potter JD, Steinmetz K (1996) Vegetables, fruit, and phytoestrogens as preventive agents. *IARC Sci Publ* 139:61–90.
19. Fernandez-Salguero PM, Ward JM, Sundberg JP, Gonzalez FJ (1997) Lesions of aryl hydrocarbon receptor-deficient mice. *Vet Pathol* 34:605–614.
20. McMillan BJ, Bradfield CA (2007) The aryl hydrocarbon receptor sans xenobiotics: Endogenous function in genetic model system. *Mol Pharmacol* 72:487–498.
21. He TC, et al. (1998) Identification of c-*MYC* as a target of the APC pathway. *Science* 281:1509–1512.
22. van Es JH, et al. (2005) Wnt signalling induces maturation of Paneth cells in intestinal crypts. *Nat Cell Biol* 7:381–386.
23. van de Wetering M, et al. (2002) The β-catenin/TCF-4 complex imposes a crypt progenitor phenotype on colorectal cancer cells. *Cell* 111:241–250.
24. Yang J, et al. (1997) Adenomatous polyposis coli (APC) differentially regulates β-catenin phosphorylation and ubiquitination in colon cancer cells. *J Biol Chem* 281:17751–17757.
25. Liu C, et al. (1999) β-Trcp couples β-catenin phosphorylation-degradation and regulates *Xenopus* axis formation. *Proc Natl Acad Sci USA* 96:6273–6278.
26. Kinzler KW, et al. (1991) Identification of FAP locus genes from chromosome 5q21. *Science* 253:661–665.
27. Nishisho I, et al. (1991) Mutations of chromosome 5q21 genes in FAP and colorectal cancer patients. *Science* 253:665–669.
28. Kinzler KW, Vogelstein B (1996) Lessons from hereditary colorectal cancer. *Cell* 87:159–170.
29. Moser AR, Pitot HC, Dove WF (1990) A dominant mutation that predisposes to multiple intestinal neoplasia in the mouse. *Science* 247:322–324.
30. Wattenberg LW (1985) Chemoprevention of cancer. *Cancer Res* 45:1–8.
31. Xu M, et al. (1996) Protection by green tea, black tea, and indole-3-carbinol against 2-amino-3-methylimidazo[4,5-*f*]quinoline-induced DNA adducts and colonic aberrant crypts in the F344 rat. *Carcinogenesis* 17:1429–1434.
32. Chen I, McDougal A, Wang F, Safe S (1998) Aryl hydrocarbon receptor-mediated antiestrogenic and antitumorigenic activity of diindolylmethane. *Carcinogenesis* 19:1631–1639.
33. Fearon ER, Vogelstein B (1990) A genetic model for colorectal tumorigenesis. *Cell* 61:759–767.
34. Reya T, Clevers H (2005) Wnt signaling in stem cells and cancer. *Nature* 434:843–850.
35. Kitagawa M, et al. (1999) An F-box protein, FWD1, mediates ubiquitin-dependent proteolysis of β-catenin. *EMBO J* 18:2401–2410.
36. Maggio-Price L, et al. (2006) *Helicobacter* infection is required for inflammation and colon cancer in Smad3-deficient mice. *Cancer Res* 66:828–838.

Journal of Steroid Biochemistry & Molecular Biology 113 (2009) 281–289

Contents lists available at ScienceDirect

Journal of Steroid Biochemistry and Molecular Biology

journal homepage: www.elsevier.com/locate/jsbmb

Comparative effects of raloxifene, tamoxifen and estradiol on human osteoblasts *in vitro*: Estrogen receptor dependent or independent pathways of raloxifene

Yasuhiro Miki[a], Takashi Suzuki[b], Shuji Nagasaki[a], Shuko Hata[a], Jun-ichi Akahira[a], Hironobu Sasano[a,*]

[a] *Department of Pathology, Tohoku University Graduate School of Medicine, 2-1 Seiryo-machi, Aoba-ku, Sendai, Miyagi 980-8575, Japan*
[b] *Department of Pathology and Histotechnology, Health Sciences, Tohoku University Graduate School of Medicine, Sendai, Japan*

ARTICLE INFO

Article history:
Received 12 August 2008
Received in revised form 20 January 2009
Accepted 20 January 2009

Keywords:
Estrogen
Osteoblasts
Osteoporosis
SERM

ABSTRACT

SERMs bind to both estrogen receptor (ER)α and β, resulting in tissue dependent estrogen agonist or antagonist responses. Both raloxifene and tamoxifen are most frequently used SERMs and exert estrogen agonistic effects on human bone tissues, but the details of their possible direct effects on human bone cells have remained largely unknown. In our present study, we examined the comparative effects of raloxifene, tamoxifen, and native estrogen, estradiol on human osteoblast cell line, hFOB *in vitro*. Both the cell numbers and the ratio of the cells in S phase fraction were significantly increased by the treatment of raloxifene or tamoxifen as well as estradiol treatments in hFOB. Gene profile patterns following treatment with raloxifene, tamoxifen, and estradiol demonstrated similar patterns in a microarray/hierarchal clustering analysis. We also examined the expression levels of these genes detected by this analysis using quantitative RT-PCR. MAF gene was induced by raloxifene treatment alone. GAS6 gene was induced by raloxifene and tamoxifen as well as estradiol. An estrogen receptor blocker, ICI 18, 286, inhibited an increase of GAS6 gene expression but not the levels of MAF gene mRNA expression. Results of our present study demonstrated that raloxifene exerted direct protective effects on human osteoblasts in both estrogen receptor dependent and independent manners.

1. Introduction

It is well known that sex steroids such as estrogen and androgen play an important role in maintenance of human bone tissues. For instance, reductions in circulating estrogen levels at the menopause are related with a rapid deterioration of bone density [1]. Various studies using experimental rodents demonstrated that estrogen depletion led to high-resorption osteoporosis caused by activation of osteoclasts which have estrogen receptor (ER)α/β mRNA or protein [2–5]. ERα/β mRNA or protein was also detected in osteoblasts [5–8]. Therefore, estrogen has considered having direct effects on osteoblasts as well as osteoclasts in human skeletal systems. Estrogen replacement therapy is very useful for bone health of postmenopausal osteoporosis patients [9] but side effects such as increased incidences of breast cancer and gynecological disorders prevented the practice of this replacement [10,11].

The selective estrogen receptor modulators (SERMs) are chemical compounds, which activate the estrogen receptors with different estrogenic and antiestrogenic tissue specific effects [12]. Results of several clinical trials demonstrated the effectiveness of raloxifene in the treatment of postmenopausal osteoporosis [13–15]. Raloxifene binds with high affinity to both ERα and ERβ as in estradiol, but in general does not increase the incidence of breast cancer and gynecological symptoms including endometrial carcinoma [16]. Results of several *in vitro* studies also demonstrated the direct effects of raloxifene on human or rodent primary osteoblast or osteoblast-like (osteosarcoma) cells [17–19]. Tamoxifen, which is also one of well-established SERMs, has been demonstrated to have partial estrogen agonistic effects on uterus as well as bone tissues [20]. In contrast to tamoxifen, raloxifene has anti-estrogenic effect on uterus as well as breast tissues [21,22]. Results of clinical trial which compared the clinical effects of raloxifene and tamoxifen on the risks of developing invasive breast carcinoma demonstrated that there were no differences between raloxifene and tamoxifen treatment groups in the total number of fracture in both hip and spine colles [15]. Results of *in vitro* study using microarray analysis demonstrated that the gene expression patterns induced by raloxifene, tamoxifen, and estradiol treatments in osteosarcoma U2OS transected with ERα (U2OS/ERα) and U2OS/ERβ [23]. However, comparative direct effects of raloxifene and tamoxifen on cell proliferation and gene expression patterns in human non-neoplastic osteoblasts have remained largely unknown.

Therefore, in this study, we first examined effects of raloxifene, tamoxifen, and estradiol on cell proliferation and cell cycle of

* Corresponding author. Tel.: +81 22 717 8050; fax: +81 22 717 8051.
E-mail address: hsasano@patholo2.med.tohoku.ac.jp (H. Sasano).

0960-0760/$ – see front matter © 2009 Elsevier Ltd. All rights reserved.
doi:10.1016/j.jsbmb.2009.01.010

normal human osteoblast-like cells. We then evaluated raloxifene, tamoxifen, and estradiol responsive genes using a microarray analysis in order to further characterize the possible differential genomic effects of these compounds on human osteoblasts. In this study, hFOB was employed in order to examine the effects on native status of human osteoblasts.

2. Materials and methods

2.1. Chemicals

Raloxifene HCl (LY139481) was kindly provided by Eli Lilly and Company (Indianapolis, IN, USA). Tamoxifen and estradiol (β-estradiol) were commercially purchased from Sigma–Aldrich Co. (MO, USA). ICI 182,780 were purchased from Tocris Cookson Inc. (MO, USA). All test materials were dissolved in dimethyl sulfoxide (DMSO; Wako Pure Chemical industries, Ltd. Osaka, Japan). The final concentrations of DMSO used in this study did not exceed 0.05% in any of the experiments preformed.

2.2. Osteoblast cell line and culture conditions

Human osteoblast cell, hFOB 1.19 cell line (CRL-11372) was obtained from American Type Culture Collection (VA, USA). hFOB 1.19 cell was cultured based on the protocol of the previously study [24]. Cells were maintained in culture at 34 °C, 95% relative humidity and 5% CO_2 in room air. The cells were plated on 96-well plates or 100 mm culture dishes at initial concentration of 5×10^4 cells/ml. Different concentrations of test compounds were added, and the assay was terminated by removing the medium from wells. ICI 182,780 was added simultaneously. In hFOB cell, expression of ERβ mRNA was more predominant than that of ERα mRNA [25].

2.3. Immunocytochemistry

Antibodies for ERα (NCL-ER-6F11) and ERβ (ER-β-14C8) were purchased from Novocastra Laboratories Ltd. (Newcastle, UK) and GeneTex, Inc. (Texas, USA), respectively. Cells were grown directly on chamber glass slides (4 well glass slide, Lab-Tek II, Nalgene Nunc International, NY, USA) under culture conditions described above. Glass slides were fixed with 10% formaldehyde for 10 min. Cells were immunostained by a biotin–streptavidin method using Histofine kit (Nichirei Co. Ltd, Tokyo, Japan) and have been previously described in detail [26]. The antigen–antibody complex was then visualized with 3,3′-diaminobenzidine solution (Dojindo Laboratories, Kumamoto, Japan). Human breast carcinoma cell line, T-47D (Cell Resource Center for Biomedical Research, Tohoku University, Sendai, Japan) was used as positive control.

2.4. Cell proliferation assay

hFOB cells were treated with steroids and test compounds after 24, 48, and 72 h when the specimens were harvested and evaluated for cell proliferation using WST-8 [2-(2-methoxy-4-nitrophenyl)-3-(4-nitrophenyl)-5-(2,4-disulfophenyl)-2H-tetrazolium, monosodium salt] method (Cell Counting Kit-8; Dojindo Laboratories). Ten microliters of 5 mM WST-8 were added to 100 l of cells, which were then incubated for 2 h at 37 °C [26]. Optical densities (OD, 450 nm) were obtained with a SpectraMax 190 microplate reader (Molecular Devices, Corp., CA, USA) and Softmax Pro 4.3 microplate analysis software (Molecular Devices, Corp.). The status of cell proliferation (%) was calculated according to the following equation: (cell OD value after test materials treated/vehicle control cell OD value) × 100.

2.5. Cell cycle analysis

In order to examine the status of cell cycle regulation of hFOB, we evaluated the percentage of cells in G0–G1, S, and G2/M phase. Cells were tripsinized and collected by centrifugation. Cells were resuspended in PBS and fixed 70% ethanol. The samples were then kept at −30 °C until use. Fixed cells were incubated with RNase (Sigma–Aldrich) for 60 min at room temperature and stained with propidium iodide (Sigma–Aldrich). Flow cytometry was then performed with FACSCalibur (BD Biosciences, San Jose, CA USA) flow cytometer. Acquisition was performed using CellQuest software (BD Biosciences) and the percentage of cells in each cell cycle phases was evaluated on a DNA linear plot using ModFit software (BD Biosciences), which counted 50,000 nuclei per sample. Mononuclear cells were used as a DNA diploid control.

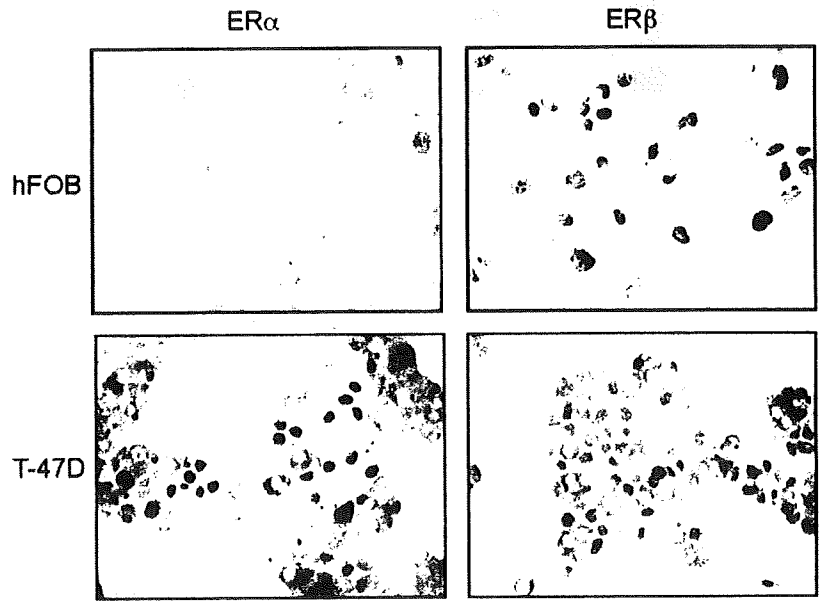

Fig. 1. Immunocytochemistry of ERα and ERβ in hFOB cells. Imunoreactivity of ERα was weak or negative in hFOB cells (*top, left*). Imunoreactivity of ERβ was markedly detected in nuclei of hFOB cells (*top, right*). Marked ERα (*bottom, left*) and weak ERβ (*bottom, right*) immunoreactivities were detected in the nuclei of T-47D cells, which is positive control of ER.

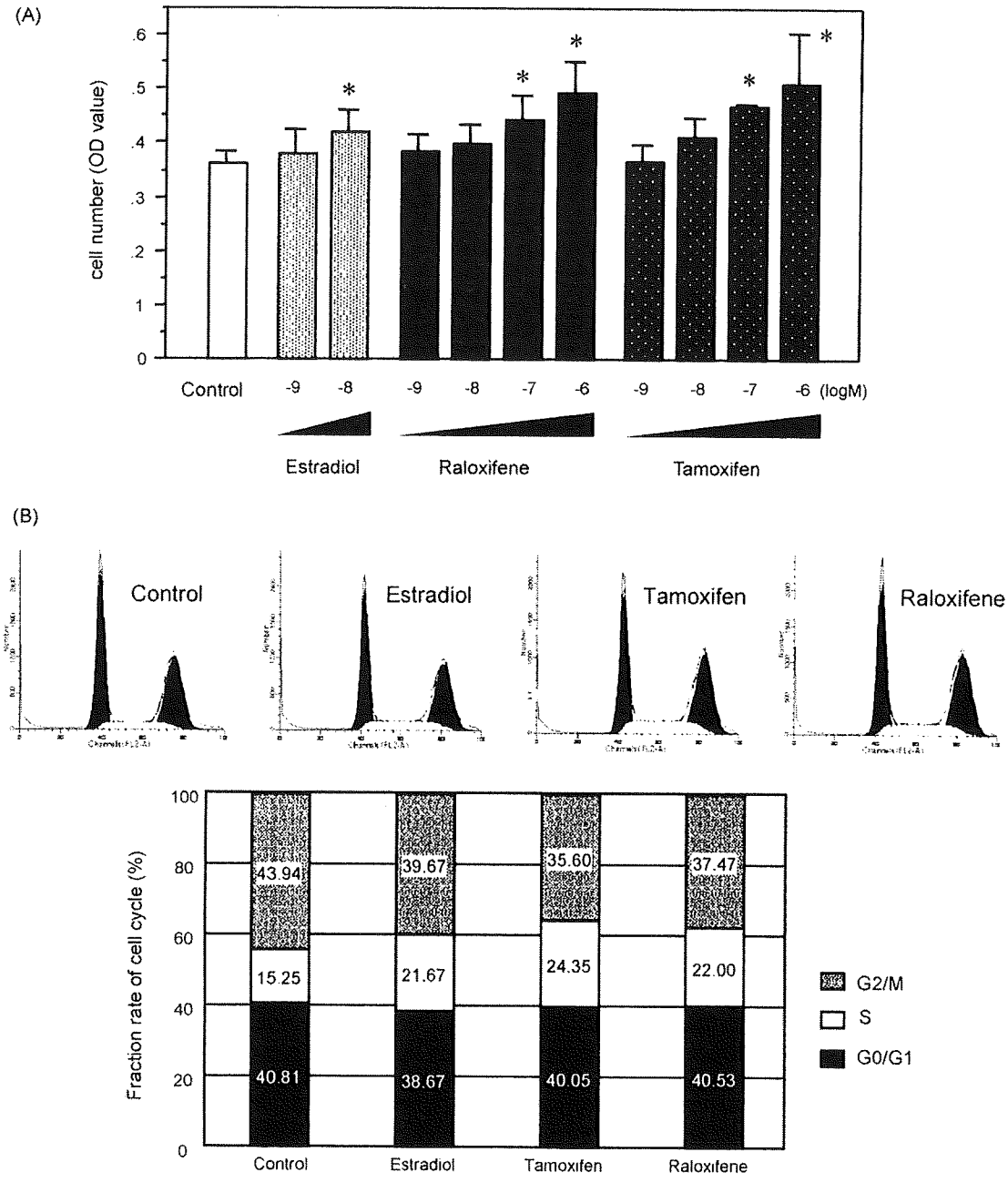

Fig. 2. A: Cell proliferation of hFOB cells treated by estradiol (10^{-9} and 10^{-8} M), raloxifene (10^{-9} to 10^{-6} M), and tamoxifen (10^{-9} to 10^{-6} M) for 72 h. All data were demonstrated as mean ($n = 3$) ± SD. $^{*}p < 0.05$ *vs.* control (0.05% DMSO). B: Cell cycle analysis of hFOB cells treated by estradiol (10^{-8} M), raloxifene (10^{-7} M), and tamoxifen (10^{-7} M) for 48 h. Similar results were obtained in at least two independent experiments.

2.6. Microarray analysis

Cell lysates were prepared using RLT buffer (QIAGEN GmbH, Hilden, Germany). Total RNA was extracted using Rneasy Mini Kit (QIAGEN). First-strand cDNA was synthesized by incubating 5 μg of total RNA with 200 U SuperScript II reverse transcriptase (Invitrogen Corporation, Carlsbad, CA, USA), 100 pmol T7-$(dT)_{24}$ primer (Invitrogen). Ten units of T4 DNA polymerase (Invitrogen) were then added, and the dsDNA was mixed with T7 RNA polymerase (Invitrogen). The purified cRNA was fragmented at 300–500 bp as target solution. Test samples and reference samples were labeled with cyanine-5 (Cy5)- and cyanine-3 (Cy3)-labeled CTP (PerkinElmer Inc., Waltham, MA, USA), respectively. Cy3- or Cy5-labeled cRNA probes were hybridized on the Human 1A ver. 2.0 (Agilent Technologies, Inc., Santa Clara, CA, USA) including 22,000 genes. The reacted arrays were then scanned as digital image files with GenePix 4000A (Axon Instruments, Foster City, CA, USA). Relative levels of gene expression were calculated by global normalization. The ratio of Cy3 and Cy5 signal intensity of each spot was quantitatively calculated using GenePix Pro 5.0 (Axon Instruments). Data were subjected to hierarchical clustering analysis and visualization using the Cluster and TreeView programs (Stanford University) [27] in order to generate tree structures based on the degree of similarity, as well as matrices comparing the levels of expression of individual genes in each sample [25].

2.7. Quantitative RT-PCR

Quantitative RT-PCR was carried out using the LightCycler System and the FastStart DNA Master SYBR Green I with

Table 1
Genes induced by raloxifene treatment in hFOB—2.0 higher or lower.

Category	GB#	Gene title	Symbol	Ratio		
				E2	TAM	RAL
Up	AF055376	v-Maf musculoaponeurotic fibrosarcoma oncogene homolog (avian)	MAF[a]	1.14	1.60	3.61
	AW006750	Kelch-like 24 (Drosophila)	DRE1	1.12	1.22	3.42
	BC030005	Multiple C2 domains, transmembrane 1	MCTP1	1.54	1.61	3.36
	AK027160	BCL2-like 11 (apoptosis facilitator)	BCL2L11[b]	1.83	1.04	3.18
	AI469884	Carboxypeptidase M	CPM[a,b]	1.63	1.90	3.11
	AL832710	Plexin D1	PLXND1	0.85	0.97	3.03
	AI479082	Growth arrest-specific 6	GAS6[a,b]	0.92	1.53	2.97
	AW504458	Guanine nucleotide binding protein (G protein), beta polypeptide 4	GNB4	1.49	1.99	2.93
	BC026009	G protein-coupled receptor 125	GPR125	1.37	0.90	2.90
	AL575337	RAB11B, member RAS oncogene family	RAB11B[a]	0.71	0.89	2.82
	AF152504	Protocadherin gamma subfamily A, 3	PCDHGA3	1.31	1.28	2.78
	AL563460	GATA binding protein 2	GATA2	1.25	0.95	2.75
	BF433902	Tumor necrosis factor receptor superfamily, member 11b (osteoprotegerin)	TNFRSF11B	0.70	0.66	0.15
Down	NM018495	Caldesmon 1	CALD1	0.88	0.50	0.16
	BC018898	Lymphotoxin beta (TNF superfamily, member 3)	LTB	1.05	0.94	0.23
	NM014421	Dickkopf homolog 2 (Xenopus laevis)	DKK2	0.59	0.63	0.24
	BC014029	Ubiquitin protein ligase E3C	UBE3C	1.07	1.10	0.29
	BE566136	Transcription factor CP2-like 2	TFCP2L2	1.02	0.77	0.30
	AL136528	Tumor protein p73	TP73	0.89	0.68	0.32
	NM006290	Tumor necrosis factor, alpha-induced protein 3	TNFAIP3	0.59	0.72	0.33
	NM000882	Interleukin 12A	IL12A	0.88	0.83	0.36
	M19701	Retinoblastoma 1 (including osteosarcoma)	RB1	0.91	1.05	0.37
	BE962027	SMAD specific E3 ubiquitin protein ligase 2	SMURF2	0.99	1.01	0.37
	H48516	Deleted in lymphocytic leukemia, 2	DLEU2	0.91	1.90	0.38

E2: estradiol, TAM: tamoxifen, RAL: raloxifene.
[a] Genes performed quantitative RT-PCR.
[b] Genes have estrogen receptor response element located its promoter lesion.

software version 3.5.3 (Roche Diagnostics GmbH, Mannheim, Germany). PCR was set up at 3 mM $MgCl_2$, 10 pmol/l of each primer. The primer positions used in this study are as follows; RPL13A (NM_012423) [25]; MAF (NM_005360), Forward 1943–Reverse 2077; RAB11B (NM_004218), Forward 289–Reverse 444; ITGB1 (NM_002211), Forward 2201–Reverse 2320; DLX (NM_005222), Forward 338–Reverse 466; PDE3B (NM_000753), Forward 443–Reverse 579; CPM (NM_001874), Forward 762–Reverse 907; GAS6 (NM_000820), Forward 1317–Reverse 1480; SAFB (NM_002967), Forward 1563–Reverse 1713; BGN (NM_001711), Forward 951–Reverse 1087; ATF7IP (NM_018179), Forward 2284–Reverse 2444; RAB40C (NM_021168), Forward 549–Reverse 741. All primer sets except for RPL13A were designed using OLIGO Primer Analysis Software (TAKARA Bio Inc., Shiga, Japan). An initial denaturing step of 95 °C for 10 min was followed by 35 cycles, respectively, of 95 °C for 10 min; 15 s annealing at 68 °C (RPL13A, MAF, DLX, GAS6, ITGB1, ATF7IP, RAB11B, RAB40C) or 64 °C (PDE3B, SAFB, CPM, BGN); and extension for 15 s at 72 °C. Negative control experiments included those lacking cDNA substrates to confirm the presence of exogenous contaminant DNA. No amplified products were detected under these conditions. The mRNA levels in each case were represented as a ratio of RPL13A, and evaluated as a ratio (%) compared with that of each control [25,26].

2.8. Statistical analysis

Results were expressed as mean ± SD. Statistical analysis was performed with the StatView 5.0 J software (SAS Institute Inc., NC, USA). All data were analyzed by analysis of variance (ANOVA) followed by post hoc Bonferroni/Dunnet multiple comparison

Table 2
Genes induced by raloxifene and tamoxifen treatment in hFOB—2.0 higher or lower.

Category	GB#	Gene title	Symbol	Ratio		
				E2	TAM	RAL
Up	AA215854	Integrin, beta 1	ITGB1[a]	0.56	3.22	3.86
	BE178502	JNK/SAPK-inhibitory kinase	JIK	1.80	3.04	3.41
	AW504458	Guanine nucleotide binding protein (G protein), beta polypeptide 4	GNB4	1.49	2.99	2.93
	NM000798	Dopamine receptor D5	DRD5	1.14	3.24	2.91
	AI769566	Scaffold attachment factor B	SAFB[a]	1.54	2.72	2.89
	NM001340	Cylicin, basic protein of sperm head cytoskeleton 2	CYLC2	1.44	2.44	2.87
	NM001531	Major histocompatibility complex, class I-related	MR1	0.99	0.25	0.29
Down	AK026133	Sema domain, immunoglobulin domain (Ig), transmembrane domain (TM) and short cytoplasmic domain, (semaphorin) 4B	SEMA4B	0.81	0.26	0.32
	AF465843	Sterile alpha motif and leucine zipper containing kinase AZK	ZAK	0.60	0.34	0.35
	BU683892	Chromobox homolog 3 (HP1 gamma homolog, Drosophila)	CBX3	0.96	0.25	0.36
	Z98752	l(3) mbt-like (Drosophila)	L3MBTL[b]	0.61	0.34	0.36

E2: estradiol, TAM: tamoxifen, RAL: raloxifene.
[a] Genes performed quantitative RT-PCR.
[b] Gene has estrogen receptor response element located its promoter lesion.

Table 3
Genes induced by raloxifene and estradiol treatment in hFOB—2.0 higher or lower.

Category	GB#	Gene Title	Symbol	Ratio		
				E2	TAM	RAL
	AA040332	Distal-less homeobox 6	DLX[a]	3.14	1.49	3.92
	D12625	Neurofibromin 1 (neurofibromatosis, von Recklinghausen disease, Watson disease)	NF1	3.05	1.19	3.34
	NM000753	Phosphodiesterase 3B, cGMP-inhibited	PDE3B[a,b]	2.87	1.36	3.29
Up	NM001711	Biglycan	BGN[a]	3.03	1.74	3.29
	NM016950	Sparc/osteonectin, cwcv and kazal-like domains proteoglycan (testican) 3	SPOCK3	2.80	1.03	2.74
	NM001145	Angiogenin, ribonuclease, RNase A family, 5	ANG	2.78	1.42	2.74
	AU156721	Pregnancy-associated plasma protein A, pappalysin 1	PAPPA	0.27	1.09	0.19
	NM003790	Tumor necrosis factor receptor superfamily, member 25	TNFRSF25	0.29	0.78	0.24
Down	BG494416	Phosphodiesterase 5A, cGMP-specific	PDE5A	0.29	0.96	0.27
	AI002966	BLZF1 and Name: basic leucine zipper nuclear factor 1 (JEM-1)	BLZF1	0.37	1.08	0.37

E2: estradiol, TAM: tamoxifen, RAL: raloxifene.
[a] Genes performed quantitative RT-PCR.
[b] Gene has estrogen receptor response element located its promoter lesion.

test. A p-value < 0.05 was considered to indicate statistical significance.

3. Results

3.1. Expressions of ERα and ERβ in hFOB cell line

Representative findings of immunocytochemistry of ERα and ERβ are illustrated in Fig. 1. Imunoreactivity of ERβ was marked in the nuclei of hFOB cells, whereas that of ERα was weak or negative in hFOB cells. Marked ERα and weak ERβ immunoreactivity was detected in the nuclei of T-47D cells.

3.2. Cell proliferation and cell cycle

Results of the cell proliferation assays are summarized in Fig. 1A. There was a significant increase in the cell number after 72 h in hFOB cells treated with 10^{-8} to 10^{-6} M estradiol (Fig. 1A). The cell number of hFOB treated by 10^{-7} to 10^{-6} M tamoxifen or raloxifene for 72 h was also significantly higher than vehicle control employed in this study.

Results of the cell cycle assays are summarized in Fig. 1B. Flow cytometry analysis demonstrated that the ratio of the cells at S fraction was significantly increased after 24 h (data not present) and 48 h (Fig. 1B) in hFOB cells treated with 10^{-7} M raloxifene, 10^{-7} M tamoxifen and 10^{-8} M estradiol, respectively.

3.3. Microarray/hierarchical clustering analysis

Results of the microarray/hierarchical clustering analysis are summarized in Fig. 2. In hFOB cells, the hierarchical clustering analysis contains 367 genes, which demonstrated expression ratios above 2.0-fold and below 0.5-fold compared with vehicle control cells after 12 h of each gene treated with 10^{-7} M raloxifene, 10^{-7} M tamoxifen, or 10^{-8} M estradiol. There were marked similarities between the expression profiles induced by raloxifene, tamoxifen and estradiol (Fig. 2A). In the hierarchical clustering analysis containing 134 genes, which demonstrated expression ratios above 2.0-fold, the expression profiles of raloxifene-treated cells were closely related to those of estradiol (Fig. 2B). In the hierarchical clustering analysis containing 231 genes, which demonstrated expression ratios below 0.5-fold, the expression profiles of tamoxifen-treated cells were also closely related to those of estradiol (Fig. 2C).

The lists of the genes with known biological functions, which demonstrated highest alterations by raloxifene, tamoxifen, and/or estradiol are summarized in Tables 1–4. The genes induced by raloxifene treatment, which were all up- or down-regulated twice or more than control are summarized in Table 1. The genes induced by raloxifene, tamoxifen and estradiol treatments, which were all up- or down-regulated twice or more than control are also summarized in Table 2 (raloxifene and tamoxifen), Table 3 (raloxifene and estradiol) and Table 4 (raloxifene, tamoxifen, and estradiol), respectively. Among these genes detected in our present study, we selected 11 genes, which were biologically known to bone homeostasis or cell proliferation after the extensive literature search. We then examined whether these 11 genes were increased by raloxifene, tamoxifen, or estradiol treatments using quantitative RT-PCR in hFOB cells. The genes which we examined using quantitative RT-PCR were as follows: MAF, CPM, GAS6, RAB11B, ITGB1, SAFB, DLX, PDE3B, BGN, ATF7IP, and RAB40C.

3.4. Validation of microarray analysis using quantitative RT-PCR

Results of the validation of microarray analysis are summarized in Fig. 3. All of these 11 genes summarized in Tables 1–4 were

Table 4
Genes induced by raloxifene, tamoxifen, and estradiol treatment in hFOB—2.0 higher or lower.

Category	GB#	Gene title	Symbol	Ratio		
				E2	TAM	RAL
	NM018005	Activating transcription factor 7 interacting protein	ATF7IP[a]	3.00	3.74	3.83
	NM006927	ST3 beta-galactoside alpha-2,3-sialyltransferase 2	SIAT4B	3.25	3.42	3.39
Up	AI955239	Oxysterol binding protein-like 7	OSBPL7	3.07	3.26	3.31
	BC014531	RAB40C and Name: RAB40C, member RAS oncogene family	RAB40C[a]	3.23	3.27	3.30
	AL137798	Macrophage stimulating 1 (hepatocyte growth factor-like)	MST1	2.15	2.80	2.76
	NM005084	Phospholipase A2, group VII (platelet-activating factor acetylhydrolase, plasma)	PLA2G7	0.05	0.16	0.14
Down	NM152573	RAS and EF-hand domain containing	RASEF	0.10	0.36	0.28
	BC036029	ADAM metallopeptidase domain 22	ADAM22	0.31	0.18	0.39

E2: estradiol, TAM: tamoxifen, RAL: raloxifene.
[a] Genes performed quantitative RT-PCR.

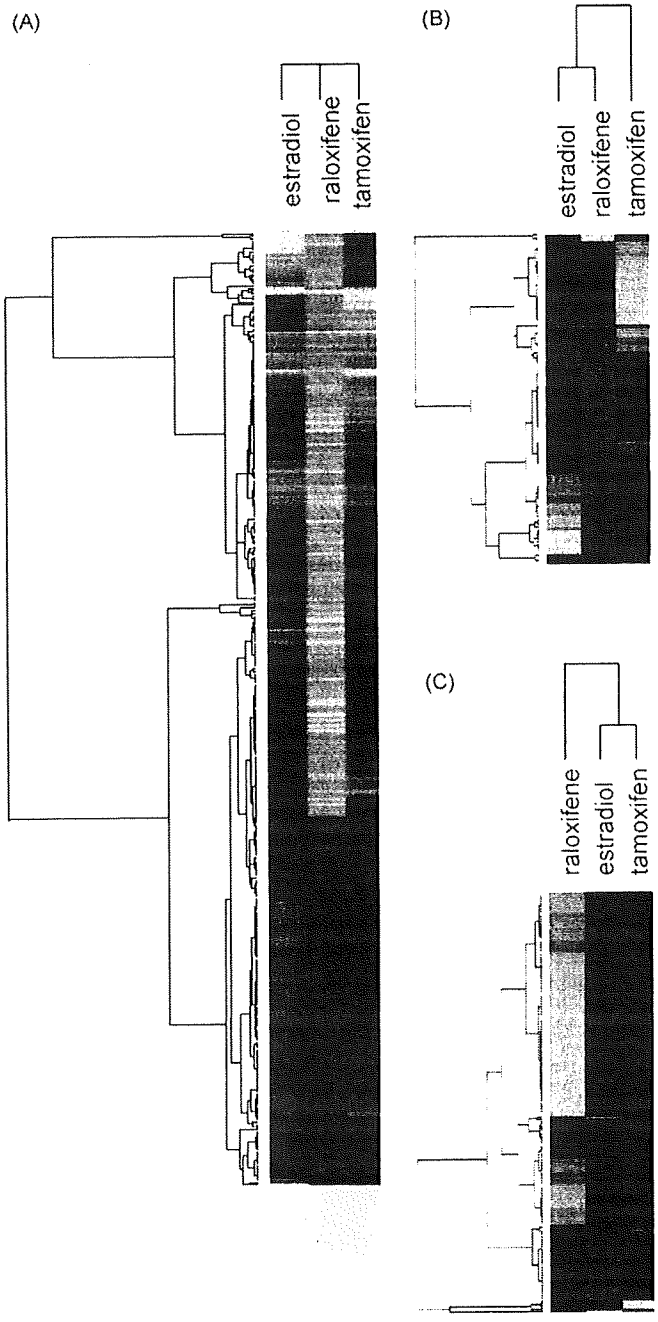

Fig. 3. In microarray/hierarchical clustering analysis of the expression levels of each genes in hFOB treated with raloxifene (10^{-7} M), tamoxifen (10^{-7} M), and estradiol (10^{-8} M) for 12 h. A: The hierarchical clustering analysis contains 367 genes, which demonstrated expression ratios above 2.0-fold and below 0.5-fold compared with vehicle control. B: The hierarchical clustering analysis contains 134 genes, which demonstrated expression ratios above 2.0-fold. C: The hierarchical clustering analysis contains 231 genes, which demonstrated expression ratios below 0.5-fold.

significantly increased by 10^{-7} M raloxifene treatment, and 3/11 genes (GAS6, ATF7TP, and RAB40C) were also significantly increased by both 10^{-7} M tamoxifen and 10^{-8} M estradiol treatments, respectively. 1/11 gene (SAFB) was also significantly increased by 10^{-7} M tamoxifen but not estradiol treatment, and 2/11 genes (DLX and PDE3B) was also significantly increased by 10^{-8} M estradiol but not tamoxifen treatment. In microarray analysis, GAS6 gene expression level did not change by tamoxifen and estradiol treatments, respectively.

3.5. *Effects of estrogen receptor blocker on hFOB treated with SERMs and estradiol*

We examined the effects of specific estrogen receptor blocker on the increases of MAF and GAS6 gene levels in hFOB treated with raloxifene, and/or tamoxifen and estradiol.

Results of the effects of estrogen receptor blocker, ICI 182,780 are summarized in Fig. 4. The cell proliferation induced by raloxifene, tamoxifen, and estradiol treatments was significantly diminished by ICI 182,780 (10^{-6} M) treatment. The increase of the GAS6 gene expression in hFOB by raloxifene, tamoxifen, and estradiol treatments was also significantly diminished by ICI 182,780 treatment. However, ICI 182,780 treatment did not influence an increase of the MAF gene expression by raloxifene treatment (Fig. 5).

4. Discussion

Results of previous studies on the gene regulation by SERMs on human osteosarcoma cell line or primary culture of osteoblasts have not necessarily been consistent. Kian et al. [23] reported that the great majority of the genes regulated in osteosarcoma U2OS/ERα in response to estradiol, raloxifene, and tamoxifen were distinct from those regulated in U2OS/ERβ in their microarray analysis. They also demonstrated that the pathways, which induced by raloxifene, and tamoxifen treatments diverge at the level of gene expression in U2OS/ERα and/ERβ, respectively [23]. Sixteen out of 30 bone homeostasis related genes were activated by three compounds, respectively in the U2OS/ERβ cells. 6/16 genes were induced by raloxifene alone, whereas 0/16 genes were co-regulated with three compounds treatments [23]. However, it is also true that the regulation patterns of the genes with an exception of 30 bone related-genes induced by raloxifene, tamoxifen, and estradiol have remained unknown. Optimal dose of estradiol employed in estrogen receptor reporter gene assay are generally considered 10 nM in *in vitro* studies, and that of raloxifene and tamoxifen are 10–100 nM in these studies [28,29]. Therefore, results of our research were considered as the pharmacological effects of estradiol and SERMs on osteoblasts *in vitro*. In our present study, however, these 30 genes reported by ERs transfected osteosarcoma cells were not up- or down-regulated in human normal osteoblasts. Both estradiol (10^{-8} to 10^{-6} M) and raloxifene (10^{-7} and 10^{-6} M) were also reported to result in a significant reduction in IL-6 production, although these effects were more pronounced with estradiol in osteosarcoma cell line (Saos-2), primary human osteoblast (HOB), and human bone marrow stromal cell line (HCC1) [30]. HOB cells were obtained from trabecular bone of four different patients (two males and two females) [30]. The study using primary human osteoblasts obtained from trabecular bone of postmenopausal woman, however, demonstrated that the effects of estradiol (10^{-8} M) or tamoxifen (10^{-8} M) did not change IL-6 expression, but raloxifene (10^{-8} M) produced a significant decrease in IL-6 mRNA expression level [31]. These discrepancies regarding down-regulation of IL-6 expression induced by SERMs and estradiol may be due to the potential differences of expression levels and patterns of ER and its isoform in human osteoblasts and its alternative osteoblast-like cells.

Therefore, in our present study, we focused on up-regulated genes induced by SERMs and estradiol using microarray analysis in hFOB osteoblasts. Over expression of MAF, which turned out to be raloxifene-specific inducible gene in our present study, selectively inhibits transcriptional activation of both IL-12 p40 and IL-12 p35 genes [32]. ERβ but not ERα are predominantly detected in osteoblasts located on human cancellous bone using immunohistochemical analysis [33]. In osteoblast-like cell lines, osteosarcoma Saos-2 and MG-63, relatively higher ERα mRNA expression was detected than that of ERβ [25]. In hFOB cell, both mRNA and protein of ERβ were more predominant than those of ERα. Therefore, hFOB

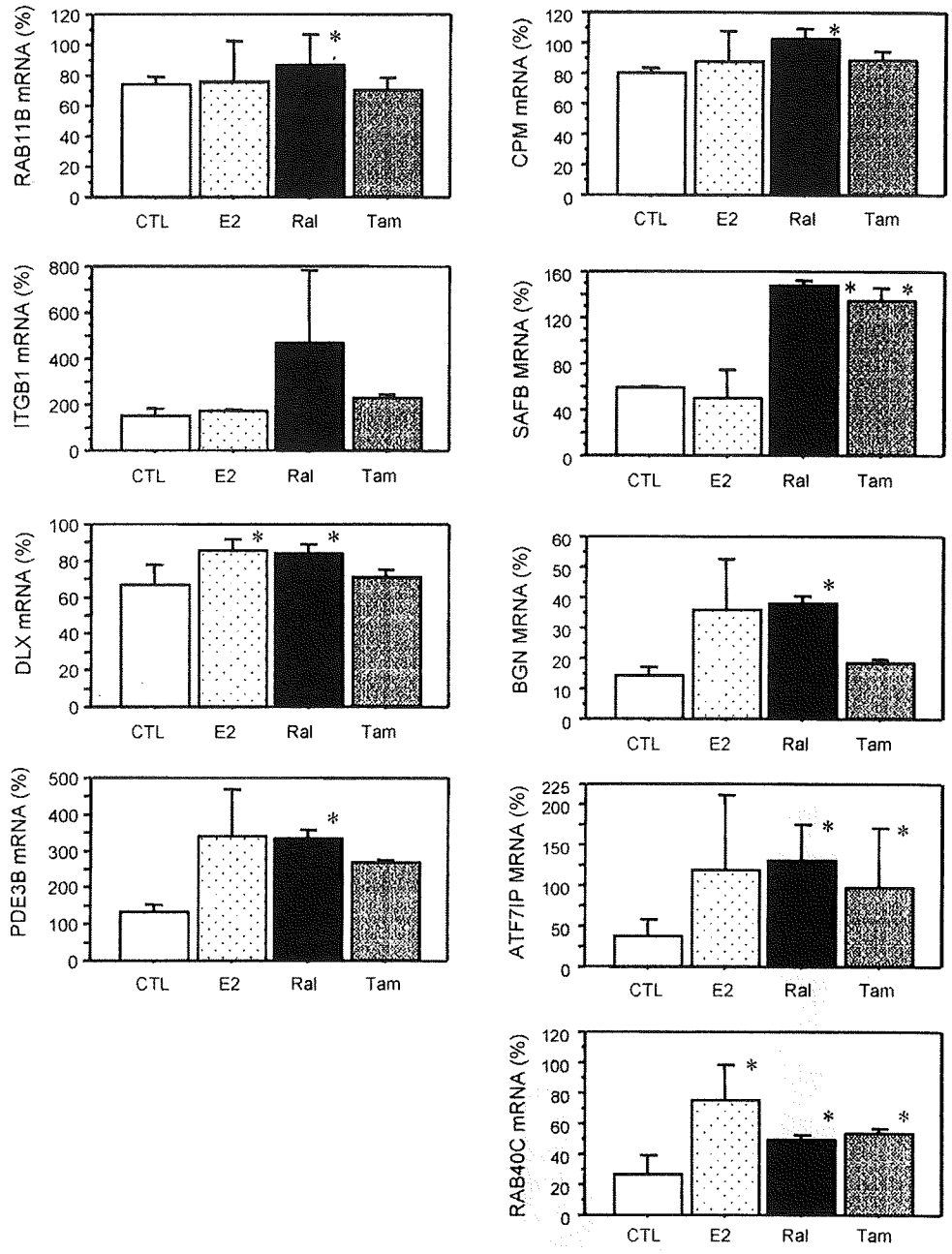

Fig. 4. Validation of microarray analysis using quantitative RT-PCR. All data were demonstrated as mean ($n = 3$) ± SD. Similar results were obtained in at least two independent experiments. CTL: vehicle (0.05% DMSO) control, E2: 10^{-8} M estradiol, RAL: 10^{-7} M raloxifene, TAM: 10^{-7} M tamoxifen, $^{*}p < 0.05$ *vs.* CTL.

examined in our present study is considered to maintain relatively native status of sex steroids pathways present in human osteoblasts and is considered suitable *in vitro* model for examining effects of steroids on human non-pathological osteoblasts.

In our present study, we focused on raloxifene-specific inducible gene, MAF and estrogen-related GAS6 genes in hFOB microarray analysis in order to further characterize the potential differences of bone-sparing effects between raloxifene and estradiol. The transcription factor MAF is required for normal chondrocyte differentiation during endochondral bone development in mice [34]. MAF was also reported to be detected in mice osteoblast [34], but its significance has still remained unclear. In multiple myeloma cells or bone marrow stroma cells, MAF up-regulates cycline D2, a promoter of cell cycle progression, and integrin β7, an adhesion molecule, respectively [35]. Therefore, MAF gene induced by only raloxifene treatment in our present study may be involved in the process of regulating cell growth or cell–cell interaction in human normal osteoblasts but it awaits further investigations for clarification. The expression of GAS6 mRNA transcript was also reported in mice osteoblasts, osteoclasts, and bone marrow cells [36]. GAS6 protein is a secreted protein originally identified as the ligand for the tyrosine kinase receptor Axl, and Gas6 was reported to be able to protect NIH3T3 cell apoptosis induced by growth factor depletion [37]. The ER-specific antagonist, ICI182,780 demonstrated no inhibitory effects on MAF expression increased by only raloxifene treatment in hFOB cells. In quantitative RT-PCR analysis, GAS6 expression was increased by raloxifene, tamoxifen, and estradiol treatments and this increase was completely inhibited by ICI182,780 treatment. GAS6 gene has estrogen response element (ERE) in its promoter lesion [38], and is considered to be primary target gene of ER in mammary epithelial cells [39]. In our present study, an increment of GAS6 mRNA levels by E2 and tamoxifen treatments could not

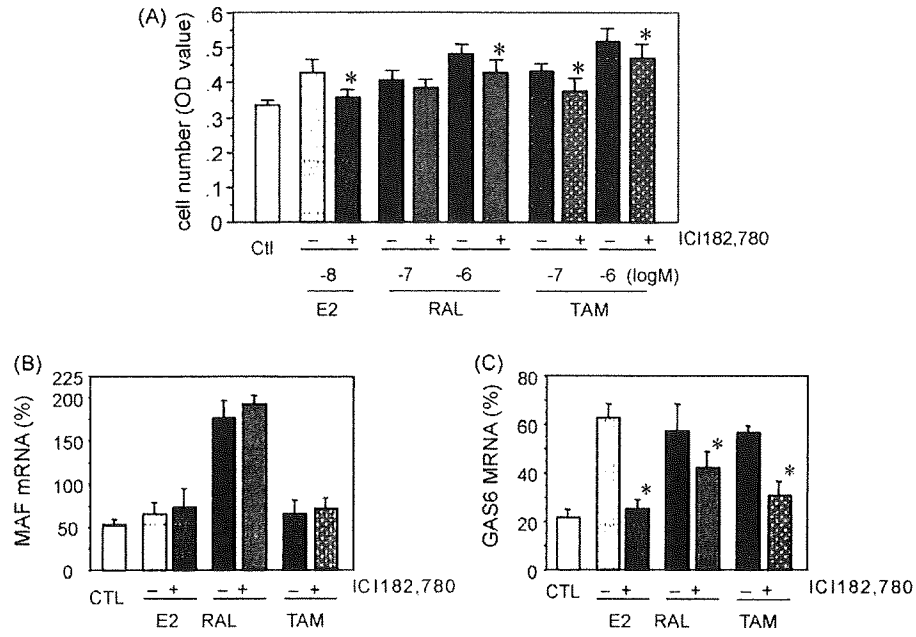

Fig. 5. A: Effects of ICI 182,780 (10^{-6} M) on raloxifene (10^{-7} and 10^{-6} M), tamoxifen (10^{-7} and 10^{-6} M), and estradiol (10^{-8} M) stimulated the cell proliferation of hFOB. B: Effects of ICI 182,780 (10^{-6} M) on MAF gene expression in hFOB. C: Effects of ICI 182,780 (10^{-6} M) on MAF gene expression in hFOB. All data were demonstrated as mean ($n=3$) ± SD. Similar results were obtained in at least two independent experiments. CTL: vehicle (0.05% DMSO) control. E2: 10^{-8} M estradiol, RAL: 10^{-7} M raloxifene, TAM: 10^{-7} M tamoxifen, +: with ICI 182,780, −: without ICI 182,780, $^{*}p < 0.05$ *vs.* CTL.

be detected using microarray analysis. This discrepancy may be explained, in part, by the greater dynamic range afforded by quantitative RT-PCR [40]. In addition, the differences in hybridization conditions for each gene-specific primer set and the corresponding cDNA target may also contribute to this discrepancy [41]. hFOB cell growth induced by raloxifene treatment was not completely inhibited by ICI182,780 treatment in our present study. These results all suggest that raloxifene may stimulate hFOB cell proliferation through both ER dependent and independent pathways such as MAF and GAS6 pathways. Endogenous estradiol metabolites induce potent biological effects through ER independent pathways in several cell lines including osteosarcoma cells [42,43]. Maran et al. [43] also reported that estradiol leads to the activation of signal transducers and activators of transcription 1 (STAT1) protein in ER negative osteoblast cell line. Furthermore, tamoxifen also has potential effects on transcriptional factors via other nuclear receptors such as steroid and xenobiotic receptor [44], which is expressed in osteoblast [45]. Results form these reports suggest that raloxifene including its metabolites may activate transcriptional factors directly in human osteoblasts. However, the mechanisms of direct effects of both MAF and GAS6 gene on hFOB cell proliferation induced by raloxifene require further investigations for clarification.

In normal bone remodeling, bone formation by osteoblasts follows bone resorption by osteoclasts and occurs in a precise and quantitative manner (coupling) [33]. In this coupling between bone formation and resorption, a coupling factor that induces bone formation is considered to be released during the process of osteoclastic bone resorption [33]. Estrogens are well known to exert pro-apoptotic effects on osteoclasts and anti-apoptotic effects on osteoblast and osteocytes [46]. This study has focused on the specific effects on osteoblast cells. However, it is true that there were significant increases in both serum bone formation and resorption markers in postmenopausal women administered with raloxifene treatment [14]. In CD14+ monocyte, tamoxifen but not raloxifene directly inhibited both human osteoclast formation and bone resorption [47]. In the co-cultures studies employing either SaOS-2 or MG-63 cells, raloxifene as well as tamoxifen inhibited osteoclast formation of CD14+ monocyte [47]. These findings as well as those of our present studies all suggest that raloxifene exert beneficial of bone-sparing effects on human bone including the modulation of an interaction between osteoblasts and osteoclasts with different pathway from tamoxifen treatment.

Acknowledgments

We appreciate Dr. Koichi Endo (Bone & Joint Field, Chugai Pharmaceutical Co., Ltd., Tokyo, Japan) for critical comments. We also appreciate Mr. Katsuhiko Ono (Department of Pathology, Tohoku University School of Medicine) for skilful technical assistances. This research was supported by research fellowships of the Japan society for the promotion of science for young scientists, risk analysis research on food and pharmaceuticals for health and labor science research grants (H19-Chemicals-004), Mitsui Life Social Welfare Foundation, and the Nakatomi Foundation.

References

[1] B.L. Riggs, S. Khosla, L.J. Melton 3rd., A unitary model for involutional osteoporosis: estrogen deficiency causes both type I and type II osteoporosis in postmenopausal women and contributes to bone loss in aging men, J. Bone Miner. Res. 13 (1998) 763–773.
[2] R.T. Turner, G.K. Wakley, K.S. Hannon, N.H. Bell, Tamoxifen inhibits osteoclast-mediated resorption of trabecular bone in ovarian hormone-deficient rats, Endocrinology 122 (1988) 1146–1150.
[3] T. Takano-Yamamoto, G.A. Rodan, Direct effects of 17 beta-estradiol on trabecular bone in ovariectomized rats, Proc. Natl. Acad. Sci. U.S.A. 87 (1990) 2172–2176.
[4] W.H. Huang, A.T. Lau, L.L. Daniels, H. Fujii, U. Seydel, D.J. Wood, J.M. Papadimitriou, M.H. Zheng, Detection of estrogen receptor alpha, carbonic anhydrase II and tartrate-resistant acid phosphatase mRNAs in putative mononuclear osteoclast precursor cells of neonatal rats by fluorescence in situ hybridization, J. Mol. Endocrinol. 20 (1998) 211–219.
[5] D. Vanderschueren, L. Vandenput, S. Boonen, M.K. Lindberg, R. Bouillon, C. Ohlsson, Androgens and bone, Endocr. Rev. 25 (2004) 389–425.
[6] O. Vidal, L.G. Kindblom, C. Ohlsson, Expression and localization of estrogen receptor-beta in murine and human bone, J. Bone Miner. Res. 14 (1999) 923–929.
[7] S. Bord, A. Horner, S. Beavan, J. Compston, Estrogen receptors alpha and beta are differentially expressed in developing human bone, J. Clin. Endocrinol. Metab. 86 (2001) 2309–2314.
[8] R. Bland, Steroid hormone receptor expression and action in bone, Clin. Sci. (Lond). 98 (2000) 217–240.

[9] D.T. Felson, Y. Zhang, M.T. Hannan, D.P. Kiel, P.W. Wilson, J.J. Anderson, The effect of postmenopausal estrogen therapy on bone density in elderly women, N. Engl. J. Med. 329 (1993) 1141–1146.
[10] D. Grady, T. Gebretsadik, K. Kerlikowske, V. Ernster, D. Petitti, Hormone replacement therapy and endometrial cancer risk: a meta-analysis, Obstet. Gynecol. 85 (1995) 304–313.
[11] S.A. Beresford, N.S. Weiss, L.F. Voigt, B. McKnight, Risk of endometrial cancer in relation to use of oestrogen combined with cyclic progestagen therapy in postmenopausal women, Lancet 349 (1997) 458–461.
[12] M. Sato, C. McClintock, J. Kim, C.H. Turner, H.U. Bryant, D. Magee, C.W. Slemenda, Dual-energy x-ray absorptiometry of raloxifene effects on the lumbar vertebrae and femora of ovariectomized rats, J. Bone Miner. Res. 9 (1994) 715–724.
[13] P.D. Delmas, N.H. Bjarnason, B.H. Mitlak, A.C. Ravoux, A.S. Shah, W.J. Huster, M. Draper, C. Christiansen, Effects of raloxifene on bone mineral density, serum cholesterol concentrations, and uterine endometrium in postmenopausal women, N. Engl. J. Med. 337 (1997) 1641–1647.
[14] B. Ettinger, D.M. Black, B.H. Mitlak, R.K. Knickerbocker, T. Nickelsen, H.K. Genant, C. Christiansen, P.D. Delmas, J.R. Zanchetta, J. Stakkestad, C.C. Gluer, K. Krueger, F.J. Cohen, S. Eckert, K.E. Ensrud, L.V. Avioli, P. Lips, S.R. Cummings, Reduction of vertebral fracture risk in postmenopausal women with osteoporosis treated with raloxifene: results from a 3-year randomized clinical trial. Multiple outcomes of raloxifene evaluation (MORE) investigators, JAMA 282 (1999) 637–645.
[15] V.G. Vogel, J.P. Costantino, D.L. Wickerham, W.M. Cronin, R.S. Cecchini, J.N. Atkins, T.B. Bevers, L. Fehrenbacher E.R.JJr., J.L. Pajon 3rd., Wadem, A. Robidoux, R.G. Margolese, J. James, S.M. Lippman, C.D. Runowicz, P.A. Ganz, S.E. Reis, W. McCaskill-Stevens, L.G. Ford, V.C. Jordan, N. Wolmark, National surgical adjuvant breast and bowel project (NSABP), Effects of tamoxifen *vs.* raloxifene on the risk of developing invasive breast cancer and other disease outcomes: the NSABP Study of Tamoxifen and Raloxifene (STAR) P-2 trial, JAMA 295 (2006) 2727–2741.
[16] H.U. Bryant, A.L. Glasebrook, N.N. Yang, M. Sato, An estrogen receptor basis for raloxifene action in bone, J. Steroid Biochem. Mol. Biol. 69 (1999) 37–44.
[17] B. Fournier, S. Haring, A.M. Kaye, D. Somjen, Stimulation of creatine kinase specific activity in human osteoblast and endometrial cells by estrogens and anti-estrogens and its modulation by calciotropic hormones, J. Endocrinol. 150 (1996) 275–285.
[18] Q. Qu, P.L. Harkonen, H.K. Vaananen, Comparative effects of estrogen and antiestrogens on differentiation of osteoblasts in mouse bone marrow culture, J. Cell Biochem. 73 (1999) 500–507.
[19] A. Taranta, M. Brama, A. Teti, V. De luca, R. Scandurra, G. Spera, D. Agnusdei, J.D. Termine, S. Migliaccio, The selective estrogen receptor modulator raloxifene regulates osteoclast and osteoblast activity *in vitro*, Bone 30 (2002) 368–376.
[20] V.C. Jordan, Effects of tamoxifen in relation to breast cancer, Br. Med. J. 1 (1977) 1534–1535.
[21] R.F. Swaby, C.G. Sharma, V.C. Jordan, SERMs for the treatment and prevention of breast cancer, Rev. Endocr. Metab. Disord. 8 (2007) 229–239.
[22] E. Barrett-Connor, Raloxifene: risks and benefits, Ann. N.Y. Acad. Sci. 949 (2001) 295–303.
[23] T.M. Kian, I. Rogatsky, C. Tzagarakis-Foster, A. Cvoro, J. An, R.J. Christy, K.R. Yamamoto, D.C. Leitman, Estradiol and selective estrogen receptor modulators differentially regulate target genes with estrogen receptors alpha and beta, Mol. Biol. Cell 15 (2004) 1262–1272.
[24] S.A. Harris, R.J. Enger, B.L. Riggs, T.C. Spelsberg, Development and characterization of a conditionally immortalized human fetal osteoblastic cell line, J. Bone Miner. Res. 10 (1995) 178–186.
[25] Y. Miki, T. Suzuki, M. Hatori, K. Igarashi, K. Aisaki, J. Kanno, Y. Nakamura, M. Uzuki, T. Sawai, H. Sasano, Effects of aromatase inhibitors on human osteoblast and osteoblast-like cells: a possible androgenic bone protective effects induced by exemestane, Bone 40 (2007) 876–887.
[26] Y. Miki, T. Suzuki, C. Tazawa, M. Ishizuka, S. Semba, I. Gorai, H. Sasano, Analysis of gene expression induced by diethylstilbestrol (DES) in human primitive Mülerian duct cells using microarray, Cancer Lett. 220 (2005) 197–210.
[27] M.B. Eisen, P.T. Spellman, P.O. Brown, D. Botstein, Cluster analysis and display of genome-wide expression patterns, Proc. Natl. Acad. Sci. U.S.A. 95 (1998) 14863–14868.
[28] L. Tou, N. Quibria, J.M. Alexander, Regulation of human cbfa1 gene transcription in osteoblasts by selective estrogen receptor modulators (SERMs), Mol. Cell Endocrinol. 183 (2001) 71–79.
[29] J.R. Schultz, L.N. Petz, A.M. Nardulli, Cell- and ligand-specific regulation of promoters containing activator protein-1 and Sp1 sites by estrogen receptors alpha and beta, J. Biol. Chem. 280 (2005) 347–354.
[30] J. Cheung, Y.T. Mak, S. Papaioannou, B.A. Evans, I. Fogelman, G. Hampson, Interleukin-6 (IL-6), IL-1, receptor activator of nuclear factor kappaB ligand (RANKL) and osteoprotegerin production by human osteoblastic cells: comparison of the effects of 17-beta oestradiol and raloxifene, J. Endocrinol. 177 (2003) 423–433.
[31] C. Mendez-Davila, C. Garcia-Moreno, C. Turbi, C. de la Piedra, Effects of 17beta-estradiol, tamoxifen and raloxifene on the protein and mRNA expression of interleukin-6, transforming growth factor-beta1 and insulin-like growth factor-1 in primary human osteoblast cultures, J. Endocrinol. Invest. 27 (2004) 904–912.
[32] S. Cao, J. Liu, M. Chesi, P.L. Bergsagel, I.C. Ho, R.P. Donnelly, X. Ma, Differential regulation of IL-12 and IL-10 gene expression in macrophages by the basic leucine zipper transcription factor c-Maf fibrosarcoma, J. Immunol. 169 (2002) 5715–5725.
[33] G.A. Rodan, L.G. Raisz, J.P. Bilezikian, Pathophysiology of osteoporosis (chapter 73), in: J.P. Bilezikian, L.G. Raisz, A. Rodan (Eds.), Principles of Bone Biology, vol. 1, 2nd ed., Academic Press, A Division of Harcourt, Inc., NY, USA, 2002, pp. 1275–1290.
[34] H.E. MacLean, J.I. Kim, M.J. Glimcher, J. Wang, H.M. Kronenberg, L.H. Glimcher, Absence of transcription factor c-maf causes abnormal terminal differentiation of hypertrophic chondrocytes during endochondral bone development, Dev. Biol. 262 (2003) 51–63.
[35] J. Kienast, W.E. Berdel, c-maf in multiple myeloma: an oncogene enhancing tumor-stroma interactions, Cancer Cell 5 (2004) 109–110.
[36] H. Kawaguchi, M. Katagiri, D. Chikazu, Osteoclastic bone resorption through receptor tyrosine kinase and extracellular signal-regulated kinase signaling in mature osteoclasts, Mod. Rheumatol. 14 (2004) 1–5.
[37] S. Goruppi, E. Ruaro, C. Schneider, Gas6, the ligand of Axl tyrosine kinase receptor, has mitogenic and survival activities for serum starved NIH3T3 fibroblasts, Oncogene 12 (1996) 471–480.
[38] V. Bourdeau, J. Deschenes, R. Metivier, Y. Nagai, D. Nguyen, N. Bretschneider, F. Gannon, J.H. White, S. Mader, Genome-wide identification of high-affinity estrogen response elements in human and mouse, Mol. Endocrinol. 18 (2004) 1411–1427.
[39] R.T. Mo, Y. Zhu, Z. Zhang, S.M. Rao, Y.J. Zhu, GAS6 is an estrogen-inducible gene in mammary epithelial cells, Biochem. Biophys. Res. Commun. 353 (2007) 189–194.
[40] S.A. Cook, T. Matsui, L. Li, A. Rosenzweig, Transcriptional effects of chronic Akt activation in the heart, J. Biol. Chem. 277 (2002) 22528–22533.
[41] K.J. Conn, M.D. Ullman, P.B. Eisenhauer, R.E. Fine, J.M. Wells, Decreased expression of the NADH:ubiquinone oxidoreductase (complex I) subunit 4 in 1-methyl-4-phenylpyridinium-treated human neuroblastoma SH-SY5Y cells, Neurosci. Lett. 306 (2001) 145–148.
[42] R.K. Dubey, E.K. Jackson, Cardiovascular protective effects of 17beta-estradiol metabolites, J. Appl. Physiol. 91 (2001) 1868–1883.
[43] A. Maran, M. Zhang, A.M. Kennedy, R.T. Turner, ER-independent actions of estrogen and estrogen metabolites in bone cells, J. Musculoskelet. Neuronal. Interact. 3 (2003).367–369.
[44] P.B. Desai, S.C. Nallani, R.S. Sane, L.B. Moore, B.J. Goodwin, D.J. Buckley, A.R. Buckley, Induction of cytochrome P450 3A4 in primary human hepatocytes and activation of the human pregnane X receptor by tamoxifen and 4-hydroxytamoxifen, Drug Metab. Dispos. 30 (2002) 608–612.
[45] T. Ichikawa, K. Horie-Inoue, K. Ikeda, B. Blumberg, S. Inoue, Steroid and xenobiotic receptor SXR mediates vitamin K2-activated transcription of extracellular matrix-related genes and collagen accumulation in osteoblastic cells, J. Biol. Chem. 281 (2006) 16927–16934.
[46] S.C. Manolagas, Birth and death of bone cells: basic regulatory mechanisms and implications for the pathogenesis and treatment of osteoporosis, Endocr. Rev. 21 (2000) 115–137.
[47] H. Michael, P.L. Harkonen, L. Kangas, H.K. Vaananen, T.A. Hentunen, Differential effects of selective oestrogen receptor modulators (SERMs) tamoxifen, ospemifene and raloxifene on human osteoclasts *in vitro*, Br. J. Pharmacol. 151 (2007) 384–395.

17β-Hydroxysteroid Dehydrogenase Type 12 in Human Breast Carcinoma: A Prognostic Factor via Potential Regulation of Fatty Acid Synthesis

Shuji Nagasaki,[1,4] Takashi Suzuki,[1,2] Yasuhiro Miki,[1] Jun-ichi Akahira,[1] Kunio Kitada,[6] Takanori Ishida,[3] Hiroshi Handa,[5] Noriaki Ohuchi,[3] and Hironobu Sasano[1]

[1]Department of Pathology, [2]Department of Pathology and Histotechnology; [3]Department of Surgical Oncology, Tohoku University Graduate School of Medicine, Sendai, Japan; [4]Kawasaki Research Center, ASKA Pharmaceutical Co., Ltd., Kawasaki, Japan; [5]Graduate School of Bioscience and Biotechnology, Tokyo Institute of Technology, Yokohama, Japan; and [6]Kamakura Research Laboratories, Chugai Pharmaceutical Co. Ltd., Kanagawa, Japan

Abstract

17β-Hydroxysteroid dehydrogenase type 12 (17β-HSD12) has been shown to be involved in elongation of very long chain fatty acid (VLCFA) as well as in biosynthesis of estradiol (E2). 17β-HSD12 expression was also reported in breast carcinomas but its functions have remained unknown. In this study, we examined the correlation between mRNA expression profiles determined by microarray analysis and tissue E2 concentrations obtained from 16 postmenopausal breast carcinoma cases. No significant correlations were detected between 17β-HSD12 expression and E2 concentration. We then immunolocalized this enzyme in 110 cases of invasive ductal carcinoma. 17β-HSD12 immunoreactivity in breast carcinoma cells was significantly associated with poor prognosis of the patients. We further examined the biological significance of 17β-HSD12 using cell-based studies. Small interfering RNA–mediated knockdown of 17β-HSD12 in SK-BR-3 (estrogen receptor–negative breast carcinoma cell line) resulted in significant growth inhibition, which was recovered by the addition of VLCFAs such as arachidonic acid. The status of 17β-HSD12 immunoreactivity was also correlated with adverse clinical outcome in cyclooxygenase 2 (COX2)–positive breast cancer patients but not in COX2-negative patients. Therefore, these findings indicated that 17β-HSD12 was not necessarily related to intratumoral E2 biosynthesis, at least in human breast carcinoma, but was rather correlated with production of VLCFAs such as arachidonic acid, which may subsequently be metabolized to prostaglandins by COX2 and result in tumor progression of the patients. [Cancer Res 2009;69(4):1392–9]

Introduction

The 17β-hydroxysteroid dehydrogenases (17β-HSD) are the key enzymes that catalyze the reversible interconversions between biologically active and inactive sex steroids (1). Fourteen isozymes of 17β-HSD have been identified and some of these isozymes have been reported to be involved in the pathogenesis or development of various hormone-dependent carcinomas (2, 3). One of the most fully characterized 17β-HSDs is type 1 (17β-HSD1), which catalyzes the conversion of weak estrone (E1) to the more potent estradiol (E2) and proposed to be involved in breast carcinoma development via E2 biosynthesis (4). In addition, some of these isozymes have been shown to have diverse substrate preferences not restricted to steroids (5).

17β-HSD type 12 (17β-HSD12) is the member of this enzyme family (Genbank accession numbers AF078850 and NM_016142; ref. 6). Moon and Horton (7) first reported that 17β-HSD12 regulate the process of very long chain fatty acid (VLCFA) elongation. Sakurai and colleagues (8) subsequently reported that 17β-HSD12 was abundantly expressed in organs involved in lipid metabolism and suggested that 17β-HSD12 plays a critical role in fatty acid synthesis. Luu-The and colleagues (6), however, subsequently reported that 17β-HSD12 catalyzes the transformation of E1 into E2. 17β-HSD12 is therefore considered to act at least as a bifunctional enzyme involved in fatty acid synthesis and/or E2 production in various tissues.

17β-HSD12 has also been shown in human breast cancer in two previous reports (9, 10). Song and colleagues (9) showed that the expression of 17β-HSD12 in human breast carcinoma was significantly higher than nonmalignant breast tissue using immunohistochemical analysis. These investigators proposed that an increased expression of 17β-HSD12 contributes to development and/or progression of breast cancer. Jansson and colleagues (10), however, reported that 17β-HSD12 mRNA levels were associated neither with survival of patients nor with any of the reported prognostic factors in estrogen receptor α (ERα)–positive breast carcinoma. They proposed that 17β-HSD12 does not play significant roles in breast cancer. The results of these two studies are not necessarily consistent and the biological significance and functions of 17β-HSD12 in human breast carcinoma have remained unknown.

Therefore, we first compared tissue E2 concentration to the 17β-HSD12 mRNA expression levels in 16 breast carcinomas based on microarray data. We further immunolocalized this enzyme in 110 cases and correlated the results with the clinical outcome of the patient. We also performed several cell-based analyses using an ERα-negative human breast cancer cell line, SK-BR-3.

Materials and Methods

Laser capture microdissection/microarray analysis. Gene expression profiles of laser capture microdissection (LCM) samples in 16 breast carcinoma cases were examined using microarray analysis. Gene expression profile data was assembled in our previous study (11). Briefly, breast

Note: Supplementary data for this article are available at Cancer Research Online (http://cancerres.aacrjournals.org/).

Requests for reprints: Hironobu Sasano, Department of Pathology, Tohoku University Graduate School of Medicine, 2-1 Seiryo-machi, Aoba-ku, Sendai, Miyagi-ken 980-8575, Japan. Phone: 81-22-717-8050; Fax: 81-22-717-8051; E-mail: hsasano@patholo2.med.tohoku.ac.jp.

doi:10.1158/0008-5472.CAN-08-0821

carcinomas were embedded in Tissue-Tek optimal cutting temperature compound (Sakura Finetechnical Co. Ltd.) and frozen sectioned at a thickness of 8 μm. Approximately 5,000 cells were laser transferred and total RNA was extracted using an RNA microisolation protocol described by Niino and colleagues (12). The mean age of the patients was 58.9 years (range, 42-74; SD, 9.9). The Committee on Ethics approved this microarray analysis, and informed consent was obtained from these patients. Sample preparation and processing were performed as described in the Affymetrix GeneChip Expression Analysis Manual (Affymetix, Inc.), with the exception that the labeled cRNA samples were hybridized to the complete human U133 GeneChip set (Affymetrix), including 22,215 and 22,577 genes. We focused on the mRNA expression of 156 genes, which is annotated according to the Gene Ontology database as the genes related to steroid biosynthetic process (accession no. 6694) and that of 17β-HSD12.

The gene expression profiles of the patients with breast cancer in which tissue estradiol was under detection limit (two patients) was averaged and applied to an analysis. Fifteen gene expression profiles of 16 breast carcinomas examined were arranged according to the levels of tissue estradiol concentration, and the clustering analysis was performed using GeneSpring GX 7.3.1 (Agilent Technologies).

Liquid chromatography/electrospray tandem mass spectrometry. Estradiol concentrations were measured by liquid chromatography (LC)/electrospray tandem mass spectrometry analysis. Briefly, breast carcinoma specimens (~40 mg for each sample) were homogenized in 1 mL of distilled water. Steroids were extracted with diethyl ether from the homogenate. The separated organic layer was evaporated, and then dissolved in picolinoic anhydride in tetrahydrofuran solution (100 μL) with triethylamine (20 μL). After application to a Bond Elute C18 column, steroid derivatives were eluted with 80% acetonitrile solution. The derivative-estradiol fraction was dissolved in the elution solvent of LC. In our study, we used a liquid chromatograph (Agilent 1100, Agilent Technologies) coupled with an API 4000 triple-stage quadrupole mass spectrometer (Applied Biosystems) operated with electron spray ionization in the positive-ion mode, and the chromatographic separation was performed on Cadenza CD-C18 column (3 × 150 mm^2, 3.5 μm; Imtakt). The injection volume was 20 μL. The mobile phase consisted of solvents A (0.1% formic acid in water, v/v) and B (acetonitrile), and delivered at flow rate of 0.4 mL/min. Total run time was 10 min. We used a mixture of solvents A and B (30:70, v/v) as an initial condition. After injection, it was followed by a linear gradient to 100% solvent B for 4 min, and this condition was maintained for 3 min. The system was returned to the initial proportion within 0.05 min and maintained for the final 2.95 min of each run. The retention times for the derived estradiol were 5.8 and 5.3 min, respectively. Ion spray voltage was 4.5 kV and the turbo gas temperature was 450°C in ionization conditions. For the multiple reaction monitoring mode, the instrument monitored the *m/z* 262 (I.S. 268) as ion produced from 383.3 (I.S. 487.2) for estradiol derivatives.

Cases for immunohistochemical analysis. One hundred ten cases of invasive ductal carcinoma of the breast were retrieved from surgical pathology files of the Department of Pathology, Tohoku University Hospital, Sendai, Japan. Breast tissue specimens were obtained from Japanese female patients who underwent mastectomy from 1988 to 2000 with a mean age of 52.9 years (range 22–81) in the Department of Surgery, Tohoku University Hospital. Any of the patients examined in our present study did not receive chemotherapy or irradiation before surgery. The mean follow-up time was 81 months (range 1–151 months). All the specimens had been fixed in 10% formalin and embedded in paraffin wax. Research protocols for this study were approved by the Ethics Committee at Tohoku University School of Medicine (approved number 2005-178).

Antibodies. Rabbit polyclonal antibody for 17β-HSD12 was raised against a peptide corresponding to the COOH-terminal residues of 17β-HSD12 (302-RAHYLKKTKKN-312). The characterization of this antibody has been previously reported by using both immunoblotting and immunohistochemistry (8). Mouse monoclonal antibody for ERα (1D5) was purchased from Immunotech. Goat polyclonal antibody for cyclo-oxygenase-2 (COX2; C-20) was purchased from Santa Cruz Biotechnology.

Immunohistochemistry. A Histofine kit (Nichirei), which uses the streptavidin-biotin amplification method, was used. Antigen retrieval for 17β-HSD12 was performed by heating the slides in a microwave oven for 15 min in the H buffer (Mitsubishi Kagaku Iatoron, Japan), and for COX2 by heating slides in an autoclave at 120°C for 5 min in citric acid buffer [2 mmol/L citric acid and 9 mmol/L trisodium citrate dehydrate (pH 6.0)]. The dilutions of the primary antibodies used were as follows: 17β-HSD12 1/500 and COX2 1/500. The antigen-antibody complex was visualized with 3,3′-diaminobenzidine solution [1 mmol/L, in 50 mmol/L Tris-HCl buffer (pH 7.6) and 0.006% H_2O_2] and counterstained with hematoxylin. As a negative control, normal rabbit or goat IgG was used instead of the primary antibodies.

Scoring of immunoreactivity. Immunoreactivity for 17β-HSD12 and COX2 was detected in the cytoplasm, and the cases that had >10% of positive carcinoma cells were considered positive, according to the method used in the previous reports (9, 13).

Cell culture. ERα-positive MCF-7 and ER-negative SK-BR-3 and MDA-MD-231 breast carcinoma cell lines were provided by the Cell Resource Center for Biomedical Research, Tohoku University (Sendai, Japan). All cell lines examined in this study were cultured in RPMI 1640 (Sigma-Aldrich) with 10% fetal bovine serum (JRH Bioscience).

Immunoblotting. The cell protein was extracted using M-PER Mammalian Protein Extraction Reagent (Pierce Biotechnology) with Halt Protease Inhibitor Cocktail (Pierce Biotechnology). The concentrations of the protein were determined using the Protein Assay Kit Wako (Wako Pure Chemical Industries). Twenty micrograms of the protein (whole cell extracts) were subjected to SDS-PAGE (10% acrylamide gel). Following SDS-PAGE, proteins were transferred onto Hybond P polyvinylidene difluoride membrane (GE Healthcare). The blots were then blocked in 5% nonfat dry skim milk for 1 h at room temperature and were then incubated with a primary antibody for ERα (DAKO), 17β-HSD12, and β-actin (Sigma-Aldrich) for 24 h at 4°C. The dilutions of primary antibodies used were as follows: 17β-HSD12 1/1,000; ERα 1/100, and β-actin 1/1,000. After incubation with anti-mouse or anti-rabbit IgG horseradish peroxidase (GE Healthcare) for 1 h at room temperature, antibody-protein complexes on the blots were detected using ECL-plus Western blotting detection reagents (GE Healthcare). The protein bands were visualized with LAS-1000 image analyzer (Fuji Photo Film Co.).

RNA interference–mediated knockdown of endogenous 17β-HSD12. Small interfering RNA (siRNA) oligonucleotides of 17β-HSD12 were used for knockdown of endogenous protein expression using Silencer Pre-designed siRNAs (Ambion), and Silencer Negative Control 1 siRNA (Ambion) was used as the negative control. The sequences of siRNA against 17β-HSD12 are as follows: ID 108811, sense 5′-GGGUAGCUAAUGACAUGAAtt-3′ and antisense 5′-UUCAUGUCAUUAGCUACCCtt-3′; ID 23823, sense 5′-GGUUUC-CAGUGAAAUAAAAtt-3′ and antisense 5′-UUUUAUUUCACUGGAAACCtg-3′. siRNAs were transfected (5 nmol/L) using HiperFect transfection reagent (Qiagen GmbH) according to the instruction manual.

Gas chromatographic analysis of fatty acids. SK-BR-3 cells were transfected with 17β-HSD12–specific siRNA (ID: 23823) or nonspecific siRNA (Silencer Negative Control 1) in a 10-cm culture dish. The medium was changed to serum-free RPMI 1640, 2 d after transfection, and subsequently cultured for 2 d. Four days after transfection (2 d after the medium was changed to serum-free condition), SK-BR-3 cells were detached from culture dishes and the number of cells was counted by the Coulter-type particle analyzer CDA-500 (Sysmex). All cells were subjected to gas chromatographic analysis. Cellular lipids were extracted with chloroform/methanol (2:1) and were hydrolyzed by 0.5 mol/L HCl (100°C, 45 min) to obtain free fatty acids. Then, free fatty acids were transesterified with 0.4 N potassium methoxide and 14% boron trifluoride in methanol. Fatty acid methyl esters were quantified with a model GC-17A gas chromatograph (Shimadzu). The data were normalized by the number of the cells applied to the analysis and represented as the amount of fatty acids of a single cell.

Cell proliferation assay. SK-BR-3 cells were transfected with 17β-HSD12–specific siRNA or nonspecific siRNA in a 96-well culture plate. In 4 d after transfection, the cell number was evaluated using a Cell counting

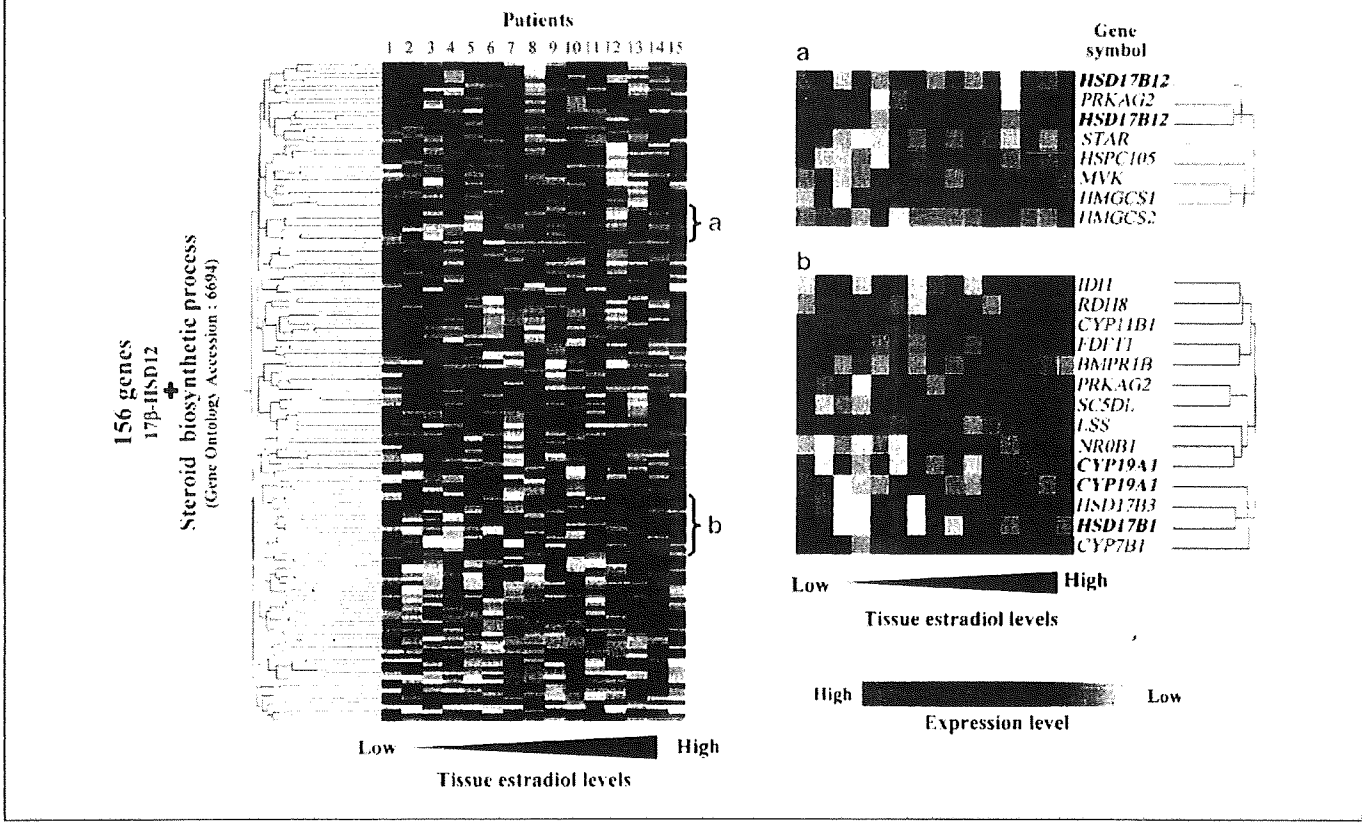

Figure 1. The comparison of gene expression profiles with tissue estradiol concentration in 16 human breast carcinoma cases. The gene expression profiles of the patients with breast carcinoma in which tissue estradiol was not detected (two patients) was averaged and applied to the analysis. In the clustering analysis, the expression profiles of 156 genes that are postulated to be involved in the steroid biosynthesis pathway and 17β-HSD12 were focused. Each case of breast carcinoma was arranged according to the levels of tissue estradiol concentration. The clusters including CYP19A and 17β-HSD1 or 17β-HSD12 are represented in detail in *a* and *b*.

kit-8 (Dojindo, Inc.) according to the instruction manual. In the assay under serum-free condition, the medium was changed at 24 h after transfection of siRNA to serum-free RPMI 1640 with or without chemically defined lipid concentrate (CDLC, Invitrogen), 10 μmol/L linoleic acid (Sigma-Aldrich), or 10 μmol/L arachidonic acid (AA; MP Biomedicals). CDLC was added to the medium in a 1/100 volume. CDLC is composed of AA, cholesterol, DL-α-tocopherol-acetate, linoleic acid, myristic acid, oleic acid, palmitoleic acid, palmitic acid, and stearic acid. Linoleic acid and AA were dissolved in DMSO and added to the culture medium. The final DMSO concentration was 0.1%.

Electron microscopy analysis. SK-BR-3 cells were transfected with 17β-HSD12–specific siRNA (ID: 23823) or nonspecific siRNA as negative control. Transmission electron microscopy (TEM) analysis was performed in these cells at 4 d after transfection. The cells were cultured and transfected with siRNAs on the Lab-Tek Chamber Slide (Nunk) and subsequently fixed with fixative solution [2% paraformaldehyde, 2.5% glutaraldehyde, 8% sucrose, 0.1 mol/L cacodylate buffer (pH 7.4)], then postfixed in cacodylate-buffered 1% osmium tetroxide, dehydrated, and embedded in Epon 812 (Structure Probe, Inc.). The ultrathin sections were stained with uranyl acetate and lead citrate and evaluated with the H7600 transmission electron microscope (Hitachi High-Technologies).

Statistical analysis. Statistical differences were examined using the StatView 5.0J software (SAS Institute). Results were expressed as mean ± SD and analyzed by Student's *t* test for gas chromatographic analysis and Bonferroni test for cell proliferation assays. Overall survival (OS) and disease-free survival (DFS) curves were generated according to the Kaplan-Meier method, and statistical significance was calculated using the log-rank test. A P value of <0.05 was considered to indicate statistical significance in all these analyses.

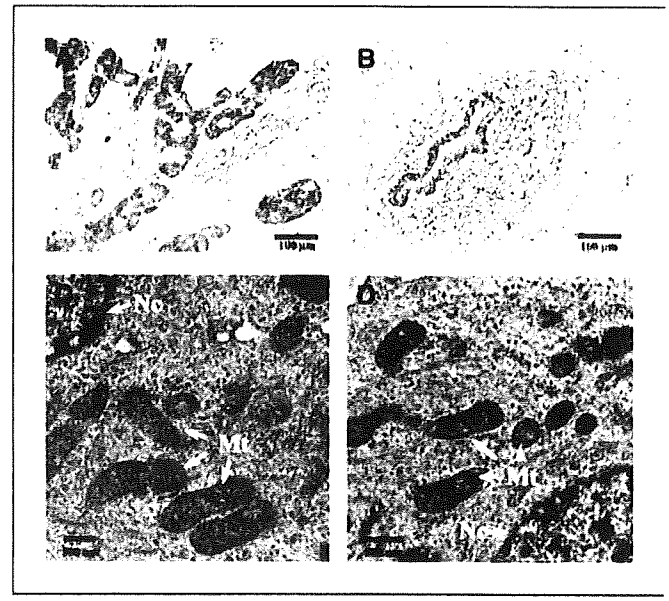

Figure 2. Immunohistochemistry of 17-HSD12 (*A* and *B*) in the cases of invasive ductal carcinoma of the breast. Marked 17β-HSD12 immunoreactivity was detected in carcinoma cells of invasive ductal carcinoma (*A*). Weak immunoreactivity for 17β-HSD12 was also detected in normal epithelial cells (*B*). TEM analysis of 17β-HSD12 knocked down SK-BR-3 cells (*C* and *D*). Structurally abnormal mitochondria were detected in 17β-HSD12 knocked down SK-BR-3 cells (*D*) compared with the negative control cells transfected with nonspecific siRNA (*C*). *Nc*, nucleus; *Mt*, mitochondrion.

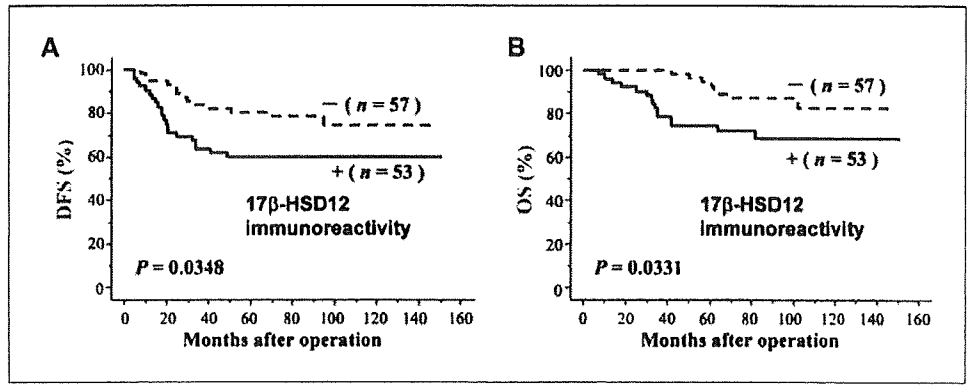

Figure 3. DFS (*A*) and OS (*B*) of 110 patients with breast carcinoma according to the status of 17β-HSD12 immunoreactivity of carcinoma cells (Kaplan-Meier method). 17β-HSD12 immunoreactivity was significantly associated with an increased risk of recurrence (P = 0.0348, log-rank test; *A*) and adverse clinical outcome of the patients (P = 0.0331, log-rank test; *B*).

Results

Comparison of gene expression profile with tissue estradiol concentrations. The data of microarray used in this study are available through the National Center for Biotechnology Information Gene Expression Omnibus database (accession GSE11965). Results of clustering analysis were summarized in Fig. 1. The abundance of 17β-HSD 1 and CYP19A1 (aromatase) mRNA tended to be positively correlated with tissue E2 levels but the 17β-HSD12 mRNA was by no means associated with the levels of tissue E2 concentration.

Immunohistochemical analysis of 17β-HSD12 in 110 invasive ductal carcinomas. 17β-HSD12 immunoreactivity was detected in 53 (48%) breast carcinoma cases. The enzyme was present in the cytoplasm of carcinoma cells (Fig. 2*A*). 17β-HSD12 immunoreactivity was also detected in epithelial cells of adjacent morphologically normal or nonneoplastic mammary glands (Fig. 2*B*), although its immunointensity was relatively weak compared with that of carcinoma cells. Immunoreactivity was also detected in human placenta tissue used as a positive control for immunohistochemistry (data not shown). Negative controls for immunostaining using nonimmunized rabbit IgG yielded no specific immunoreactivity (data not shown).

Correlation between 17β-HSD12 immunoreactivity and clinical outcomes in 110 invasive ductal carcinomas. DFS and OS curves were shown in Fig. 3. The statistical analysis showed that the status of 17β-HSD12 in breast carcinoma was significantly associated with poor survival of the patient (DFS: P = 0.0348, OS: P = 0.0331).

ERα and 17β-HSD12 protein expression in MCF-7, SK-BR-3, and MDA-MB-231. The protein expression levels of ERα and 17β-HSD12 were examined in three carcinoma cell lines (Fig. 4*A*). ERα protein was detected in MCF-7 but not in SK-BR-3 and MDA-MB-231. A single distinct band of 17β-HSD12 protein at the protein size 32 kDa was detected in MCF-7 and SK-BR-3 cells, whereas in MDA-MB-231, the intensity of the band was relatively weak.

RNAi-mediated knockdown of 17β-HSD12 in SK-BR-3 cells. The decreased amounts of 17β-HSD12 protein were detected by immunoblot analysis 3 days after the transfection of specific siRNA (Fig. 4*B*). The knockdown effects were also confirmed 4 days after the transfection (data not shown). There were no significant differences between protein expression levels of the two negative control groups treated with or without nonspecific siRNA.

Gas chromatographic analysis of fatty acids. The result of the gas chromatographic analysis was shown in Fig. 4*C* to *D*. Each fatty

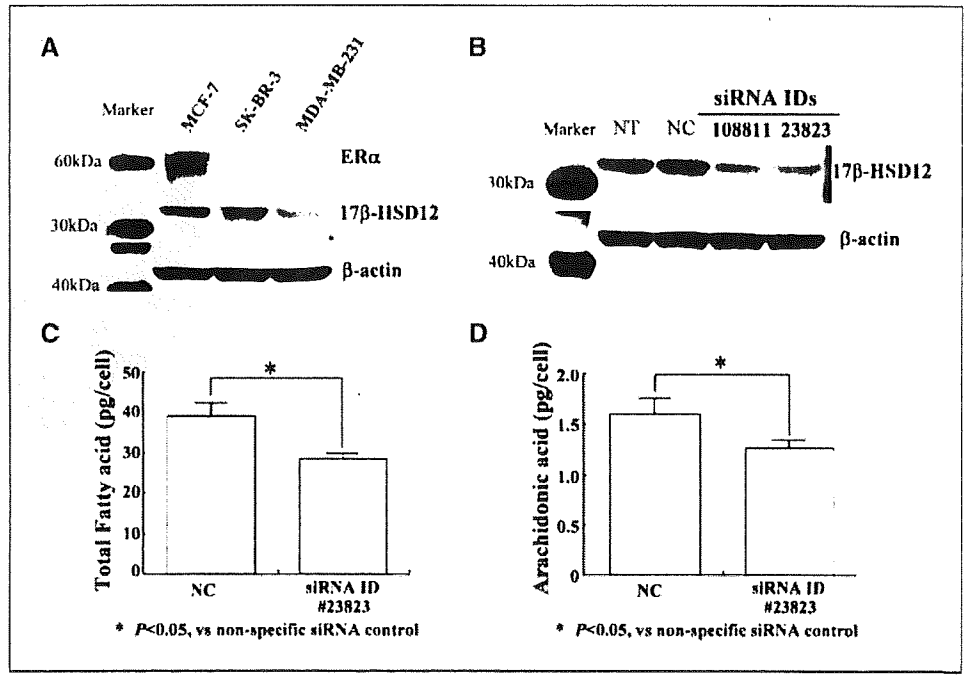

Figure 4. Immunoblotting for ERα and 17β-HSD12 in human breast carcinoma cell lines (*A* and *B*). ERα immunoreactivity (~66 kDa) was detected in MCF-7 but not in SK-BR-3 and MDA-MB-231 (*A*). Immunoreactivity of 17β-HSD12 (~32 kDa) was detected in all cell lines but that in MDA-MB-231 was weak (*A*). siRNA-mediated knockdown of 17β-HSD12 in SK-BR-3 (*B*). 17β-HSD12 immunoreactivity was clearly diminished in cells treated with 17β-HSD12–specific siRNA compared with two negative control cells (*NT*, treated with reagent only; *NC*, transfected with nonspecific siRNA) 3 d after transfection. Gas chromatographic analysis of fatty acids in cells treated with 17β-HSD12–specific siRNA (*C* and *D*). Total fatty acid and AA levels of cells treated with 17β-HSD12–specific siRNA (23823) was significantly lower than that of the negative control cells.

acid contents in both groups were summarized in Supplementary Table S1. The total amounts of fatty acid (TFA) and AA are as follows (pg/cell): negative control cells (TFA, 39.12 ± 3.45; AA, 1.61 ± 0.16); 17β-HSD12 knocked down cells (using siRNA 23823; TFA, 28.54 ± 1.42; AA, 1.27 ± 0.07). TFA and AA levels of 17β-HSD12 knocked down cells (23823) were significantly lower (27.0% and 21.1%) than those of negative controls. The TFA and AA in the cell transfected with siRNA (108811) was also decreased in the same manner but the decrement did not reach statistical significance (Supplementary Fig. S1).

Cell proliferation assay. The significant growth inhibition was detected in SK-BR-3 cells transfected with two distinct 17β-HSD12–specific siRNAs compared with those transfected with nonspecific siRNA (NC) under conditions of serum addition (Fig. 5*A*). The growth inhibition detected in knocked down SK-BR-3 cells, however, became more pronounced and statistically significant compared with the NC group under serum-free conditions (Fig. 5*A*). The growth inhibition detected in the serum-free condition was partially recovered by the addition of CDLC or linoleic acid (LA; Fig. 5*B* and *C*), but was completely reversed by the addition of AA (Fig. 5*D*). This growth recovery by AA was detected in a dose-dependent manner (Supplementary Fig. S2).

Correlation between 17β-HSD12 immunoreactivity and clinical outcomes of the groups divided according to COX2 status. We examined the effect of 17β-HSD12 expression in the survival of the patient in correlation with COX2 status, which has been reported as the main enzyme converting AA to prostaglandins and subsequently stimulates cancer progression, based on the result of cell proliferation assay in which AA is considered the key fatty acid synthesized via the pathway including 17β-HSD12. The COX2 status was significantly associated with reduced DFS (P = 0.0279; Fig. 6*A*) in all the patients. In COX2-positive cases, the status of 17β-HSD12 immunoreactivity was significantly associated with reduced DFS (P = 0.0371; Fig. 6*B*) and OS (P = 0.0389, data not shown), but not in the COX2-negative groups [DFS (P = 0.5166; Fig. 6*C*) and OS (P = 0.4278, data not shown)].

Electron microscopic analysis. The structure of cristae assembled by the inner mitochondrial membrane was clearly detected in the mitochondria of the negative control cells (Fig. 2*C*), whereas these cristae were more obscure or unclear in 17β-HSD12 knocked down SK-BR-3 (Fig. 2*D*).

Discussion

In our present study, the comparison between microarray clustering analysis and tissue E2 concentrations in breast carcinoma showed the correlation of relative abundance of estrogen-producing or metabolizing enzymes such as 17β-HSD1

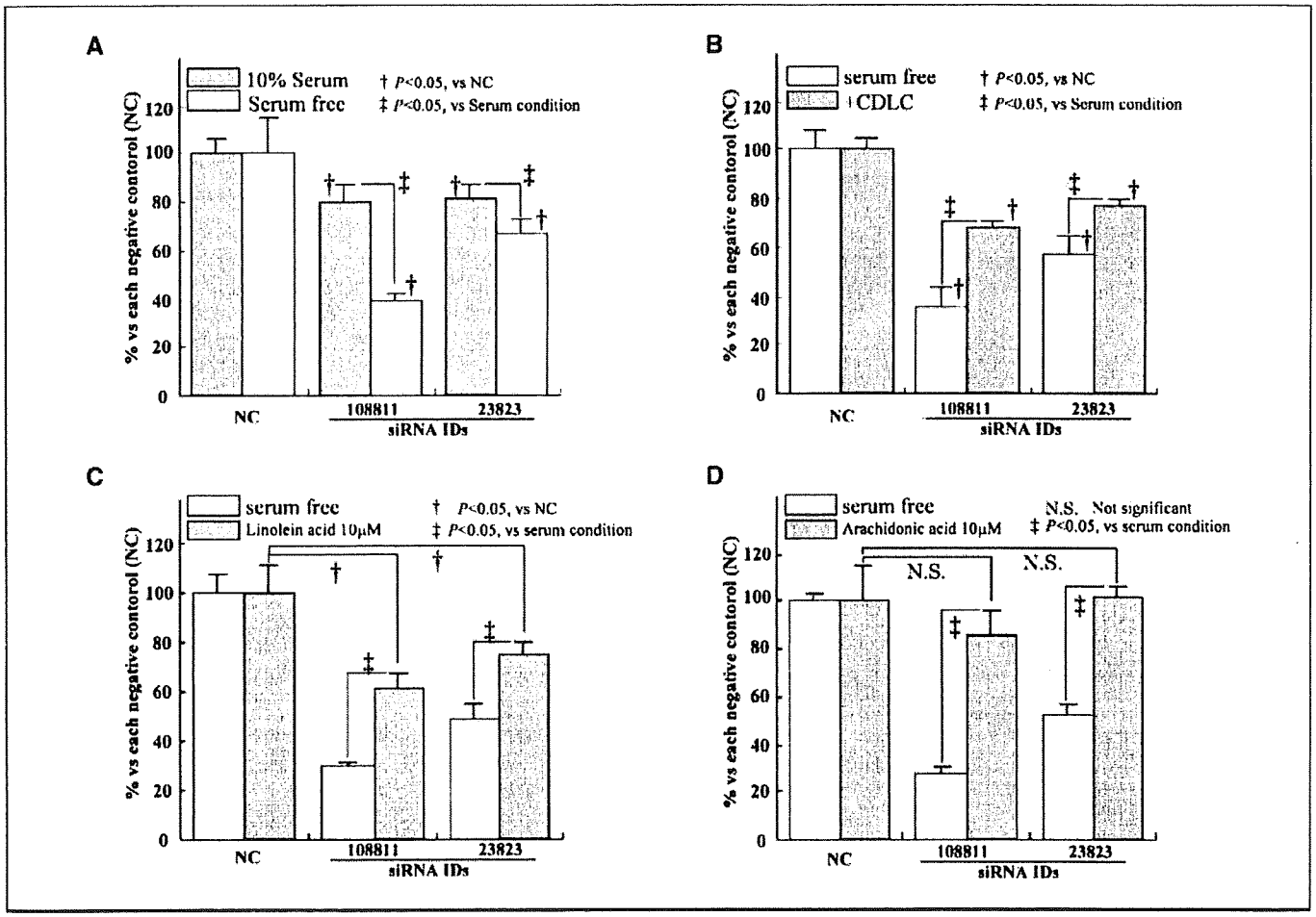

Figure 5. Growth inhibition of SK-BR-3 induced by 17β-HSD12 knockdown. Cell proliferation of SK-BR-3 was significantly inhibited by 17β-HSD12 knockdown compared with negative controls with or without serum in the culture medium (*A*). The inhibition of cell proliferation mediated by this 17β-HSD12 knockdown was partly recovered by addition of CDLC (*B*) and linoleic acid (*C*), but completely reversed by addition of AA (*D*). *Columns*, mean (n = 4); *bars*, SD.

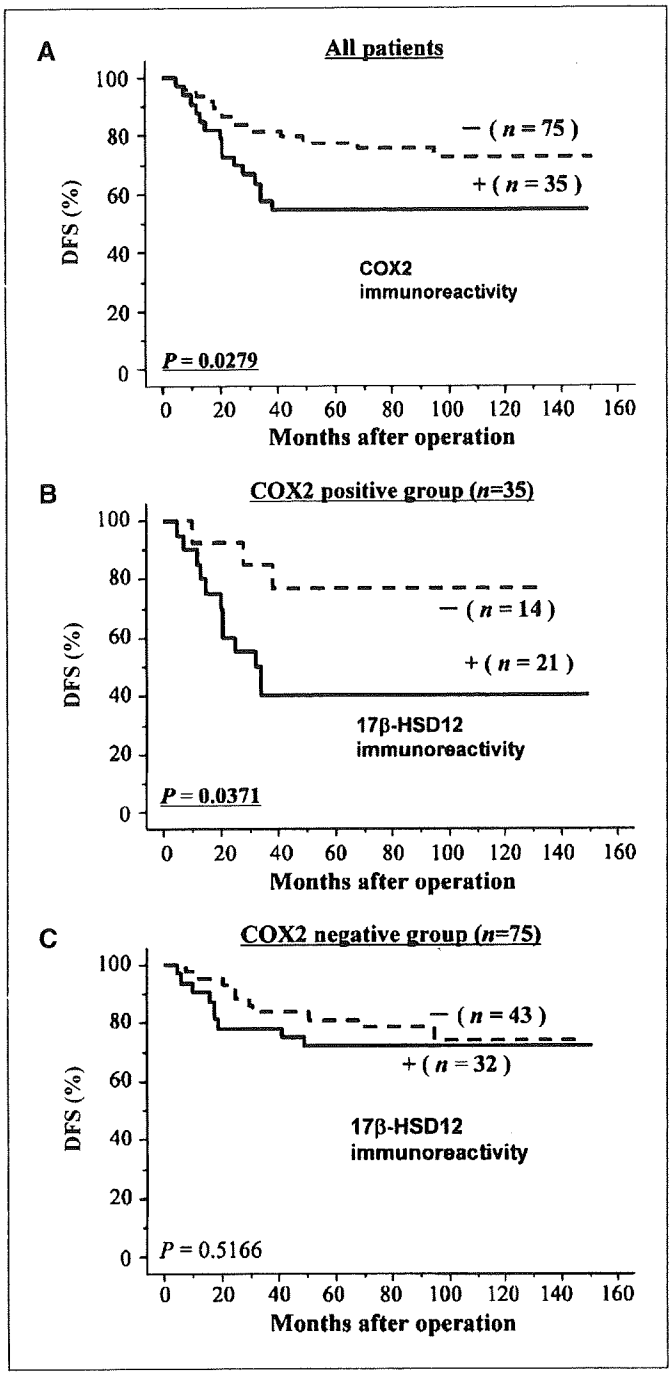

Figure 6. DFS of 110 patients with breast carcinoma according to the status of COX2 and 17β-HSD12 immunoreactivity of carcinoma cells (Kaplan-Meier method). COX2 immunoreactivity was significantly associated with DFS (P = 0.0279, log-rank test; *A*). 17β-HSD12 immunoreactivity was significantly associated with the DFS (P = 0.0371, log-rank test) in the COX2-positive cases (*B*), but not in the COX2-negative cases (*C*).

or aromatase with intratumoral estrogen concentrations as expected. 17β-HSD12, however, was not only located in the different clusters of the enzymes above but was not at all correlated with the tissue E2 levels (Fig. 1). These findings suggest that 17β-HSD12 in breast carcinoma cells contributes to a metabolic pathway other than *in situ* E2 biosynthesis. Day and colleagues (14) also showed that 17β-HSD12 was highly expressed in breast cancer cell lines, but its enzymatic activity of E1 to E2 was not altered in 17β-HSD12 knocked down cells transfected with specific siRNA. They concluded that 17β-HSD12 may play a role other than E2 biosynthesis in these tumor cells, such as fatty acid elongation. This finding by Day and colleagues is also consistent with the above-mentioned hypothesis in our present study.

In immunohistochemical analysis, the patients positive for this enzyme were significantly associated with poor clinical outcome (Fig. 3); however, there were no significant associations between the status of 17β-HSD12 immunoreactivity and clinicopathologic variables, including patient's age, menopausal status, clinical stages, tumor size, lymph node status, histologic grade, ERα status, HER2 status, and Ki-67 LI status (data not shown). Therefore, we further evaluated the potential factors that may account for the aggressive clinical behavior of 17β-HSD12–positive breast carcinoma patients using several cell-based *in vitro* studies.

We first performed siRNA-mediated gene knockdown assay. The ER-negative breast cancer cell line SK-BR-3 (15) was selected to eliminate the potential effects of estrogenic signals. In addition, the 17β-HSD12 protein expression in the SK-BR-3 cell was relatively higher than the other ER-negative cell line, MDA-MB-231 (Fig. 4*A*). The results of the knockdown assay showed a slight but significant inhibition of cell proliferation on the knocked down cells cultured in the medium supplemented with serum (Fig. 5*A*). The growth-inhibitory effects became more pronounced in the serum-free condition (Fig. 5*A*) and were partly recovered by supplementation of CDLC (Fig. 5*B*). CDLC contains ω-6 fatty acids, such as LA and AA, which had been widely recognized to enhance the risk of breast cancer (16). In addition, LA and AA have also been reported to stimulate breast cancer cell proliferation (17, 18). We thus focused on these two fatty acids in our present study. The growth inhibition of knocked down cells was partly recovered by the addition of LA (Fig. 5*C*), but completely recovered by the addition of AA (Fig. 5*D*). Therefore, the growth inhibition of cells under the serum-free condition is reasonably postulated to result from deprivation of fatty acids, such as AA, normally supplied by the *de novo* fatty acid synthesis reaction in the cells including 17β-HSD12. In addition, the results of the gas chromatographic analysis in which the amounts of almost all fatty acids were significantly decreased in 17β-HSD12 knocked down SK-BR-3 (Fig. 4*C*) strongly support the hypothesis described above. VLCFA have been shown to play an important role in a wide range of biological functions (19–24). In particular, AA is generally considered more important than other VLCFAs in various aspects of cancer cell biology (19–24). These data all indicated that AA is one of the key fatty acids synthesized via the pathway involving 17β-HSD12 and that AA stimulates breast cancer cell proliferation.

In knockdown assays, the treatment with siRNA 108811 resulted in the marked decrement of cell proliferation compared with that with siRNA 23823 (Fig. 5). Slight induction of caspase-3/7 activity was also detected by treatment with siRNA 108811, but not by siRNA 23823 (data not shown). Therefore, the treatment with siRNA 108811 is considered to induce weak off-target effects related to apoptosis, and we mainly used siRNA 23823 for another knockdown assay including gas chromatographic analysis and electron microscopic analysis in our present study. 17β-HSD12 is considered to be involved in VLCFA(C>18) synthesis (25) but a significant decrement in the amounts of lauric acid (C12:0), myristic acid (C14:0), palmitic acid (C16:0), and palmitoleic acid (C16:1ω7), which is considered to be mainly synthesized by FASN (26), was detected. These results also suggest that the metabolism

of these fatty acids was accelerated to compensate the depletion of VLCFA induced by 17β-HSD12 knockdown. Further investigations are, however, required to clarify which types of fatty acids are mainly synthesized by the pathway involving 17β-HSD12.

AA is enzymatically converted to prostaglandins by cyclooxygenases, especially by COX2 present in carcinoma cells, and is considered to exert diverse biological functions, including cancer cell progression (27, 28). In addition, COX2 expression is reported to be correlated with worse prognosis of the patient with breast cancer (Fig. 6*A*; refs. 29, 30). We therefore further categorized all cases into two groups (COX2 positive and negative) according to the result of immunohistochemistry of COX2, and the potential effects of 17β-HSD12 were analyzed by the Kaplan-Meier method. 17β-HSD12 immunoreactivity was significantly associated with decreased DFS (Fig. 6*B*) and OS (data not shown) in the COX2-positive group of the patients but not in the COX2-negative group (Fig. 6*C*). These findings also suggest that AA is considered to be at least one of the VLCFAs synthesized via the pathways involving 17β-HSD12 and further metabolized to prostaglandins by the COX2 pathway, which may contribute to the poor clinical outcome of the patients.

Fatty acid is also well known as a major component of the cell membrane, and fatty acid synthase was reported to be abundantly expressed in various common human malignancies (31–40). Therefore, the deprivation of fatty acid synthesis by 17β-HSD12 knockdown is considered to result in the abnormalities of the membrane of organelle and/or cell surface. Results of TEM analysis showed that ultrastructural abnormalities of mitochondrial cristae were detected in the knocked down cells (Fig. 2*D*), which suggests that VLCFAs synthesized via the pathway involving 17β-HSD12 may be introduced to a newly formed mitochondrial inner membrane and may influence the cell proliferation. In addition, we performed scanning electron microscopic analysis but no differences were discernible between the cell surface of knocked down and negative control cells (data not shown).

In conclusion, the findings in our present study indicate that the expression of 17β-HSD12 is not necessarily involved in peripheral E2 biosynthesis in human breast carcinoma, but is involved in the growth of carcinoma cells, possibly via the biosynthesis pathway of VLCFAs such as AA, and contributes to breast carcinoma progression.

Disclosure of Potential Conflicts of Interest

No potential conflicts of interest were disclosed.

Acknowledgments

Received 3/4/2008; revised 10/19/2008; accepted 11/3/2008; published OnlineFirst 02/03/2009.

Grant support: Japanese Ministry of Health, Labour and Welfare for Researches on Intractable Diseases, Risk Analysis Research on Food and Pharmaceuticals, and Development of Multidisciplinary Treatment Algorithm with Biomarkers and Modeling of the Decision-making Process with Artificial Intelligence for Primary Breast Cancer. This work was also partly supported by Grant-in-Aid for Scientific Research (18390109) from the Japanese Ministry of Education, Culture, Sports, Science and Technology, and the Yasuda Medical Foundation.

The costs of publication of this article were defrayed in part by the payment of page charges. This article must therefore be hereby marked *advertisement* in accordance with 18 U.S.C. Section 1734 solely to indicate this fact.

We thank Dr. Nobuyuki Sakurai (Department of Obstetrics and Gynecology, Keio University School of Medicine, Shinjuku-ku, Tokyo, Japan) for providing antibody against 17β-HSD12.

References

1. Labrie F, Luu-The V, Lin SX, et al. Intracrinology: role of the family of 17 β-hydroxysteroid dehydrogenases in human physiology and disease. J Mol Endocrinol 2000; 25:1–16.
2. Suzuki T, Miki Y, Nakamura Y, et al. Sex steroid-producing enzymes in human breast cancer. Endocr Relat Cancer 2005;12:701–20.
3. Nakamura Y, Suzuki T, Nakabayashi M, et al. *In situ* androgen producing enzymes in human prostate cancer. Endocr Relat Cancer 2005;12:101–7.
4. Suzuki T, Moriya T, Ariga N, Kaneko C, Kanazawa M, Sasano H. 17β-hydroxysteroid dehydrogenase type 1 and type 2 in human breast carcinoma: a correlation to clinicopathological parameters. Br J Cancer 2000;82: 518–23.
5. Moeller G, Adamski J. Multifunctionality of human 17β-hydroxysteroid dehydrogenases. Mol Cell Endocrinol 2006;248:47–55.
6. Luu-The V, Tremblay P, Labrie F. Characterization of type 12 17β-hydroxysteroid dehydrogenase, an isoform of type 3 17β-hydroxysteroid dehydrogenase responsible for estradiol formation in women. Mol Endocrinol 2006; 20:437–43.
7. Moon YA, Horton JD. Identification of two mammalian reductases involved in the two-carbon fatty acyl elongation cascade. J Biol Chem 2003;278:7335–43.
8. Sakurai N, Miki Y, Suzuki T, et al. Systemic distribution and tissue localizations of human 17β-hydroxysteroid dehydrogenase type 12. J Steroid Biochem Mol Biol 2006; 99:174–81.
9. Song D, Liu G, Luu-The V, et al. Expression of aromatase and 17β-hydroxysteroid dehydrogenase types 1, 7 and 12 in breast cancer. An immunocytochemical study. J Steroid Biochem Mol Biol 2006;101:136–44.
10. Jansson AK, Gunnarsson C, Cohen M, Sivik T, Stal O. 17β-Hydroxysteroid dehydrogenase 14 affects estradiol levels in breast cancer cells and is a prognostic marker in estrogen receptor-positive breast cancer. Cancer Res 2006;66:11471–7.
11. Miki Y, Suzuki T, Kitada K, et al. Expression of the steroid and xenobiotic receptor and its possible target gene, organic anion transporting polypeptide-A, in human breast carcinoma. Cancer Res 2006;66:535–42.
12. Niino YS, Irie T, Takaishi M, et al. PKCθ II, a new isoform of protein kinase C specifically expressed in the seminiferous tubules of mouse testis. J Biol Chem 2001; 276:36711–7.
13. Suzuki T, Hayashi S, Miki Y, et al. Peroxisome proliferator-activated receptor γ in human breast carcinoma: a modulator of estrogenic actions. Endocr Relat Cancer 2006;13:233–50.
14. Day JM, Foster PA, Tutill HJ et al. 17β-hydroxysteroid dehydrogenase Type 1, and not Type 12, is a target for endocrine therapy of hormone-dependent breast cancer. Int J Cancer 2008;122:1931–40.
15. Tong D, Schuster E, Seifert M, Czerwenka K, Leodolte S, Zeillinger R. Expression of estrogen receptor β isoforms in human breast cancer tissues and cell lines. Breast Cancer Res Treat 2002;71:249–55.
16. Rose DP. Effects of dietary fatty acids on breast and prostate cancers: evidence from in vitro experiments and animal studies. Am J Clin Nutr 1997;66:1513–22S.
17. Reyes N, Reyes I, Tiwari R, Geliebter J. Effect of linoleic acid on proliferation and gene expression in the breast cancer cell line T47D. Cancer Lett 2004;209:25–35.
18. Bazanamahefa L, Prouff S, Bardon S. Stimulatory effect of arachidonic acid on T-47D human breast cancer cell growth is associated with enhancement of cyclin D1 mRNA expression. Nutr Cancer 2000;38:274–80.
19. Schneiter R, Hitomi M, Ivessa AS, Fasch EV, Kohlwein SD, Tartakoff AM. A yeast acetyl coenzyme A carboxylase mutant links very-long-chain fatty acid synthesis to the structure and function of the nuclear membrane-pore complex. Mol Cell Biol 1996;16:7161–72.
20. Schneiter R, Brugger B, Amann CM, et al. Identification and biophysical characterization of a very-long-chain-fatty-acid-substituted phosphatidylinositol in yeast subcellular membranes. Biochem J 2004; 381:941–9.
21. McMahon A, Butovich IA, Mata NL, et al. Retinal pathology and skin barrier defect in mice carrying a Stargardt disease-3 mutation in elongase of very long chain fatty acids-4. Mol Vis 2007;13:258–72.
22. Vasireddy V, Uchida Y, Salem N, Jr., et al. Loss of functional ELOVL4 depletes very long-chain fatty acids (> or = C28) and the unique ω-*O*-acylceramides in skin leading to neonatal death. Hum Mol Genet 2007;16:471–82.
23. Leonard AE, Kelder B, Bobik EG, et al. Identification and expression of mammalian long-chain PUFA elongation enzymes. Lipids 2002;37:733–40.
24. Poulos A, Beckman K, Johnson DW, et al. Very long-chain fatty acids in peroxisomal disease. Adv Exp Med Biol 1992;318:331–40.
25. Jakobsson A, Westerberg R, Jacobsson A. Fatty acid elongases in mammals: their regulation and roles in metabolism. Prog Lipid Res 2006;45:237–49.
26. Smith S. The animal fatty acid synthase: one gene, one polypeptide, seven enzymes. FASEB J 1994;8:1248–59.
27. Wang D, DuBois RN. Cyclooxygenase 2-derived prostaglandin E2 regulates the angiogenic switch. Proc Natl Acad Sci U S A 2004;101:415–6.
28. Chang SH, Liu CH, Conway R, et al. Role of prostaglandin E2-dependent angiogenic switch in cyclooxygenase 2-induced breast cancer progression. Proc Natl Acad Sci U S A 2004;101:591–6.
29. Ristimaki A, Sivula A, Lundin J, et al. Prognostic significance of elevated cyclooxygenase-2 expression in breast cancer. Cancer Res 2002;62:632–5.
30. Witton CJ, Hawe SJ, Cooke TG, Bartlett JM. Cyclooxygenase 2 (COX2) expression is associated with poor outcome in ER-negative, but not ER-positive, breast cancer. Histopathology 2004;45:47–54.
31. Alo' PL, Visca P, Marci A, Mangoni A, Botti C, Di Tondo U. Expression of fatty acid synthase (FAS) as a predictor of recurrence in stage I breast carcinoma patients. Cancer 1996;77:474–82.
32. Epstein JI, Carmichael M, Partin AW. OA-519 (fatty acid synthase) as an independent predictor of pathologic

state in adenocarcinoma of the prostate. Urology 1995;45:81–6.
33. Gansler TS, Hardman W III, Hunt DA, Schaffel S, Hennigar RA. Increased expression of fatty acid synthase (OA-519) in ovarian neoplasms predicts shorter survival. Hum Pathol 1997;28:686–92.
34. Innocenzi D, Alo PL, Balzani A, et al. Fatty acid synthase expression in melanoma. J Cutan Pathol 2003;30:23–8.
35. Krontiras H, Roye GD, Beenken SE, et al. Fatty acid synthase expression is increased in neoplastic lesions of the oral tongue. Head Neck 1999;21:325–9.
36. Kusakabe T, Nashimoto A, Honma K, Suzuki T. Fatty acid synthase is highly expressed in carcinoma, adenoma and in regenerative epithelium and intestinal metaplasia of the stomach. Histopathology 2002;40:71–9.
37. Piyathilake CJ, Frost AR, Manne U, et al. The expression of fatty acid synthase (FASE) is an early event in the development and progression of squamous cell carcinoma of the lung. Hum Pathol 2000;31:1068–73.
38. Rashid A, Pizer ES, Moga M, et al. Elevated expression of fatty acid synthase and fatty acid synthetic activity in colorectal neoplasia. Am J Pathol 1997;150:201–8.
39. Shurbaji MS, Kalbfleisch JH, Thurmond TS. Immunohistochemical detection of a fatty acid synthase (OA-519) as a predictor of progression of prostate cancer. Hum Pathol 1996;27:917–21.
40. Camassei FD, Jenkner A, Rava L, et al. Expression of the lipogenic enzyme fatty acid synthase (FAS) as a predictor of poor outcome in nephroblastoma: an interinstitutional study. Med Pediatr Oncol 2003;40:302–8.

Chicken ovalbumin upstream promoter transcription factor II in human breast carcinoma: Possible regulator of lymphangiogenesis via vascular endothelial growth factor-C expression

Shuji Nagasaki,[1,3] Takashi Suzuki,[1,2] Yasuhiro Miki,[1] Jun-ichi Akahira,[1] Hirotaka Shibata,[4] Takanori Ishida,[5] Noriaki Ohuchi[5] and Hironobu Sasano[1,6]

[1]Department of Pathology, Tohoku University Graduate School of Medicine, [2]Department of Pathology and Histotechnology, Tohoku University Graduate School of Medicine, 2-1 Seiryo-machi, Aoba-ku, Sendai, Miyagi, 980-8575; [3]Kawasaki Research Center, ASKA Pharmaceutical, 1604 Simosakunobe, Takatu-ku, Kawasaki, Kanagawa, 213-8522; [4]Department of Internal Medicine, School of Medicine, Keio University, 35 Shinanomachi, Shinjuku-ku, Tokyo, 160-8582; [5]Department of Surgical Oncology, Tohoku University Graduate School of Medicine, 1-1 Seiryo-machi, Aoba-ku, Sendai, Miyagi, 980-8574, Japan

(Received August 20, 2008/Revised December 6, 2008/Accepted December 8, 2008/Online publication January 13, 2009)

Chicken ovalbumin upstream promoter transcription factors (COUP-TF) are orphan members of the nuclear receptor superfamily and consist of COUP-TFI and COUP-TFII. COUP-TFI was reported to be overexpressed in human breast cancer and to promote estrogen-independent transcriptional activity of estrogen receptor α. COUP-TFII, however, has not been examined in the breast. Therefore, we carried out immunohistochemical analysis of COUP-TFII in human breast cancer in order to clarify its biological and clinical significance. We immunolocalized COUP-TFII in 119 human breast cancers and correlated the findings with various clinicopathological parameters. Fifty-nine percent of the cases were immunohistochemically positive for COUP-TFII. COUP-TFII positivity was correlated with poor clinical outcome, and a statistically significant correlation was detected between COUP-TFII and the following clinicopathological parameters: clinical stage, lymph node status, histological grade, and estrogen receptor α status. In addition, short interfering RNA-mediated knockdown of COUP-TFII in the breast carcinoma cell line MCF-7 decreased the level of vascular endothelial growth factor-C mRNA expression, which is a known inducer of lymphangiogenesis and lymph node metastasis. These results suggest that COUP-TFII is involved in the development of advanced human breast cancer. (*Cancer Sci* 2009; 100: 639–645)

Chicken ovalbumin upstream promoter transcription factors are orphan members of the nuclear receptor superfamily.[1] They belong to the steroid and thyroid hormone superfamily of nuclear receptors and are involved in regulating the expression of various genes.[1] COUP-TF were initially characterized in chick oviduct[2] and HeLa extracts,[3] where they bind as dimers to the COUP element of the ovalbumin gene promoter to activate transcription.[2] COUP-TF were therefore initially characterized as transcriptional activators of the chicken ovalbumin gene but are currently also considered as repressors of the transcriptional activity of other nuclear hormone receptors[4] such as retinoic acid receptor, thyroid hormone receptor, peroxisome proliferator-activated receptor, and vitamin D receptor, via direct interaction, competing for their DNA binding sites, or by heterodimerization with retinoid X receptor.[5,6] There are two COUP-TF genes reported in mammals, *COUP-TFI* and *COUP-TFII*. These two COUP-TF genes are closely correlated, with an overall amino acid identity of 87%. They are evolutionarily conserved in the DNA binding domain as well as the ligand-binding domain, which suggests that they are relatively primordial members of the nuclear receptor family and have important biological functions.[7]

In human breast cancer, the expression of COUP-TFI was reported to be increased in carcinoma cells compared with normal cells and to promote estrogen-independent transcriptional activity of ERα.[8,9] Therefore, the expression of COUP-TFI in ERα-positive breast cancer is reasonably postulated to be involved in its progression. In addition, high amounts of COUP-TFII expression were reported in invasive lung carcinoma cell lines[10] and in dedifferentiated endometrial[11] and ovarian cancer cell lines.[12] All of these reporteds findings suggest that COUP-TFII expression may affect breast cancer cell progression through modulation of other nuclear receptors such as ERα, as well as COUP-TFI, or through other pathways. However, the clinical significance of COUP-TFII in breast carcinoma remains virtually unknown.

Therefore, in the present study, we examined the immunolocalization of COU-TFII in 119 cases of human breast carcinoma, and correlated these findings with various clinicopathological parameters in order to clarify the biological and clinical significance of this orphan nuclear receptor in human breast cancer progression. In addition, we examined the potential regulation of VEGF-C mRNA expression by COUP-TFII using the breast carcinoma cell line MCF-7 and the siRNA-mediated knockdown method.

Materials and Methods

Patients and tissue preparation. 119 specimens of invasive ductal carcinoma of the breast were retrieved from the pathology archives of the Department of Surgery, Tohoku University Hospital, Sendai, Japan. Breast tissue specimens were obtained from female patients with a mean age of 53.2 years (range 22–81 years) who underwent mastectomy from 1988 to 2000. The patients did not receive chemotherapy or irradiation prior to surgery. 67 of the patients received tamoxifen therapy after surgery. The median follow-up time was 94 months (range 3–151 months). The histological grade of each specimen was

[6]To whom correspondence should be addressed.
E-mail: hsasano@patholo2.med.tohoku.ac.jp

Abbreviations: ANG, angiopoietin; COUP-TF, chicken ovalbumin upstream promoter transcription factor; DFS, disease-free survival; ER, estrogen receptor; HER, human epidermal growth factor receptor; LI, labeling index; OS, overall survival; PR, progesterone receptor; RT, reverse transcription; PCR, polymerase chain reaction; SDS-PAGE, sodium dodecylsulfate–polyacrylamide gel electrophoresis; siRNA, short interfering RNA; VEGF, vascular endothelial growth factor; VEGFR, vascular endothelial growth factor receptor.

doi: 10.1111/j.1349-7006.2008.01078.x

evaluated based on the method of Elston and Ellis.[13] All of the specimens had been fixed with 10% formalin and embedded in paraffin wax. The research protocols for this study were approved by the Ethics Committee at Tohoku University School of Medicine (approval number 2004-146).

Antibodies. Mouse monoclonal antibody for COUP-TFII (H7147), ERα (1D5), PR (MAB429), and Ki-67 (MIB1) were purchased from Perseus Proteomics (Tokyo, Japan), Immunotech (Marseille, France), Chemicon (Temecula, CA, USA) and Dako (Copenhagen, Denmark), respectively. Rabbit polyclonal antibody for HER-2/*neu* (A0485) was purchased from Dako.

Immunohistochemistry. A Histofine Kit (Nichirei, Tokyo, Japan), which uses the streptavidin–biotin amplification method, was used for immunostaining in this study. Antigen retrieval for COUP-TFII, ERα, PR, Ki-67, and HER-2/*neu* was carried out by heating the slides in an autoclave at 120°C for 5 min in citric acid buffer (2 mM citric acid and 9 mM trisodium citrate dehydrate, pH 6.0). The dilutions of the primary antibodies used in this study were as follows: COUP-TFII, 1/250; ERα, 1/50; PR, 1/30; Ki-67, 1/100; and HER2/neu, 1/200. The antigen–antibody complexes were visualized with 3,3′-diaminobenzidine solution (1 mM, in 50 mM Tris-HCl buffer, pH 7.6, and 0.006% H_2O_2), and counterstained with hematoxylin. Adrenal gland was used as a positive control for COUP-TFII. As a negative control, normal, rabbit, or mouse IgG (subclass-matched) was used instead of the primary antibodies.

Scoring of immunoreactivity. Immunoreactivity for COUP-TFII, ERα, PR, and Ki-67 was detected in the nucleus. Immunoreactivity was evaluated in more than 1000 carcinoma cells, and moderately or highly immunostained cells were counted for all of the antigens examined. The percentage of immunoreactivity (i.e. LI) was subsequently obtained. For ERα, PR, and Ki-67, cases with a LI of more than 10% were determined to be positive.[14–16] For the analysis evaluating the possible correlation between COUP-TFII status and clinical outcome, the cases were classified into three different groups according to COUP-TFII LI (++, >50% LI; +, 10–49% LI; and –, 0–9% LI). Subsequently, survival curve analysis according to the Kaplan–Meier method and univariate or multivariate analyses were carried out. HER2 score was also evaluated as follows: 0, none; 1+, faint and focal membrane staining of the tumor; 2+, moderate membrane staining of >10% of the tumor; and 3+, intense membrane staining of >10% of the tumor. Cases of 3+ were considered positive in the present study.

Cell culture. The human breast carcinoma cell line MCF-7 was provided by the Cell Resource Center for Biomedical Research, Tohoku University (Sendai, Japan). MCF-7 cells were cultured in RPMI-1640 (Sigma-Aldrich, St Louis, MO, USA) with 10% fetal bovine serum (JRH Bioscience, Lenexa, KS, USA).

RNA interference-mediated knockdown of endogenous COUP-TFII. siRNA oligonucleotides of COUP-TFII were used for the knockdown of endogenous protein expression using Silencer Pre-designed siRNA (Ambion, Austin, TX, USA), and Silencer Negative Control#1 siRNA (Ambion) was used as a negative control. The siRNA sequences against COUP-TFII are summarized as follows: ID 5922, sense 5′-GGCCAUAGUCCUGUUCACCtt-3′ and antisense 5′-GGUGAACAGGACUAUGGCCtt-3′; ID 139844, sense 5′-GGAACCACAUAUAACACUUtt-3′ and antisense 5′-AAGUGUUAUAUGUGGUUCCtc-3′. siRNA (10 nM) was transfected using HiperFect transfection reagent (Qiagen, Hilden, Germany) according to the instruction manual.

Immunoblotting. The cell protein was extracted using M-PER Mammalian Protein Extraction Reagent (Pierce Biotechnology, Rockford, IL, USA) with Halt Protease Inhibitor Cocktail (Pierce Biotechnology) 3 days after siRNA transfection. The protein concentrations were determined using a protein assay kit (Wako Pure Chemical Industries, Osaka, Japan). The whole-cell extracts (20 μg of the protein) were subjected to SDS-PAGE (10% acrylamide gel). Following SDS-PAGE, proteins were transferred onto Hybond P polyvinylidene difluoride membranes (GE Healthcare, Buckinghamshire, UK). The blots were then blocked in 5% non-fat dry skim milk for 1 h at room temperature, and were subsequently incubated with a primary antibody for COUP-TFII or β-actin (Sigma-Aldrich) for 24 h at 4°C. The dilutions of primary antibodies used were as follows: COUP-TFII, 1/1000; β-actin, 1/1000. After incubation with anti-mouse IgG–horseradish peroxidase (GE Healthcare) for 1 h at room temperature, antibody–protein complexes on the blots were detected using ECL-plus western blotting detection reagents (GE Healthcare). The protein bands were then visualized using an LAS-1000 image analyzer (Fuji Photo Film, Tokyo, Japan).

Reverse transcription–polymerase chain reaction analysis. Total RNA was extracted using TRIzol Reagent (Invitrogen Carlsbad, CA, USA) 3 days after siRNA transfection, and cDNA was synthesized using a QuantiTect reverse transcription kit (Qiagen). Real-time PCR was carried out using the LightCycler System and FastStart DNA Master SYBR Green I (Roche Diagnostics, Mannheim Germany). The PCR primer sequence of VEGF-C and the ribosomal protein L13A (RPL13A) used in the present study were as follows: VEGF-C (NM_005429), forward 5′-CAAGGCCCCAAACCAGTA-3′ and reverse 5′-GTCTTGTTCGCTGCCTGA-3′; RPL13A (NM_012423), forward 5′-CCTGGAGGAGAAGAGGAAAGAGA-3′ and reverse 5′-TTGAGGACCTCTGTGTATTTGTCAA-3′. cDNA of known VEGF-C concentration, and the housekeeping gene *RPL13A* were used to generate standard curves for real-time quantitative PCR in order to determine the quantity of target cDNA transcript. The mRNA level in each case was represented as a ratio of RLP13A and was evaluated as a ratio (%) compared with the control.

Statistical analysis. Statistical differences were examined using StatView 5.0 J software (SAS Institute, Cary, NC, USA). In the comparison study between COUP-TFII immunoreactivity and several clinicopathological parameters, COUP-TFII LI was used because no rational thresholds were presented so far, and the value was demonstrated as the mean ± SEM. The statistical analyses of COUP-TFII LI between dichotomous groups, such as menopausal status, tumor size, lymph node status, ERα status, PR status, Ki-67 status, and HER2 status, were carried out using the Mann–Whitney *U*-test. ANOVA and Fisher's Protected Least Significant Difference (PLSD) test were also used for multiple comparisons of COUP-TFII LI among each group of different clinical stages and histological grades, and the *P*-values obtained were subjected to Bonferroni's correction. OS and DFS curves were generated according to the Kaplan–Meier method by classifying all of the patients into '++' and '– or +' groups, and statistical significance was calculated using the log-rank test. Cox's proportional hazards model was used for univariate and multivariate analyses using the dichotomous groups of COUP-TFII LI described above. A value of $P < 0.05$ was considered statistically significant.

Results

Immunohistochemical analysis of COUP-TFII in 119 human breast carcinomas. COUP-TFII immunoreactivity was detected in the nuclei of carcinoma cells (Fig. 1c,d). COUP-TFII immunoreactivity was also detected in scattered foci of normal epithelial cells adjacent to the carcinoma but its relative immunointensity was markedly low compared to in carcinoma cells (Fig. 1b). The number of cases with immunopositive COUP-TFII in each group was summarized as follows: –, 49 cases (41.2%); +, 44 cases (37.0%); and ++, 26 cases (21.8%).

Correlation between COUP-TFII immunoreactivity and clinical outcome in the 119 patients. DFS and OS curves for the three groups of patients according to COUP-TFII status (–, +, and ++) demonstrated a positive correlation between COUP-TFII status

doi: 10.1111/j.1349-7006.2008.01078.x